

Electronic Supporting Information

Synthesis and characterization of Al and Si substituted Polyoxometalates

Jan-Christian Raabe^{1,2}, Saurabh Chitnis², and Maximilian J. Poller¹

¹Institute for Technical and Macromolecular Chemistry, Universität Hamburg,
Bundesstraße 45, 20146 Hamburg, Germany

JanChristian.Raabe@uni-hamburg.de

Maximilian.Poller@uni-hamburg.de

²Department of Chemistry, Dalhousie University, Coburg Road 6274, 15000 Halifax, Nova
Scotia, Canada

Jan-Christian.Raabe@dal.ca

Saurabh.Chitnis@dal.ca

Contents

1	Polyoxometalates	3
2	Experimental part	5
2.1	Chemicals	5
2.2	Experimental procedures	6
2.2.1	Synthesis of TBA ₉ [PW ₉ O ₃₄]	6
2.2.2	Synthesis of TBA ₂ WO ₄	6
2.2.3	Synthesis of TBA ₃ [PW ₁₂ O ₄₀]	7
2.2.4	Synthesis of TBA ₆ [PAIW ₁₁ O ₄₀]	7
2.2.5	Synthesis of TBA ₅ [PSiW ₁₁ O ₄₀]	8
2.2.6	Reactivity study	8
2.3	Characterization	10
2.3.1	Compositional analysis	10
2.3.2	Vibrational Spectroscopy	12
2.3.3	Crystallography	16
2.3.4	NMR Spectroscopy	20
2.3.5	Electrochemical Analysis	32
2.4	Computational chemistry	35
3	Literature	41

1 Polyoxometalates

Oxo ligands in terminal or bridging coordination motif, Figure S1:

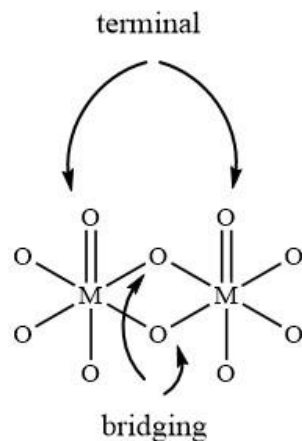


Figure S1: Coordination of the oxo ligand. Terminal $M=O_t$ and bridging $M-O-M$.

Different POM structure-types, Figure S2:

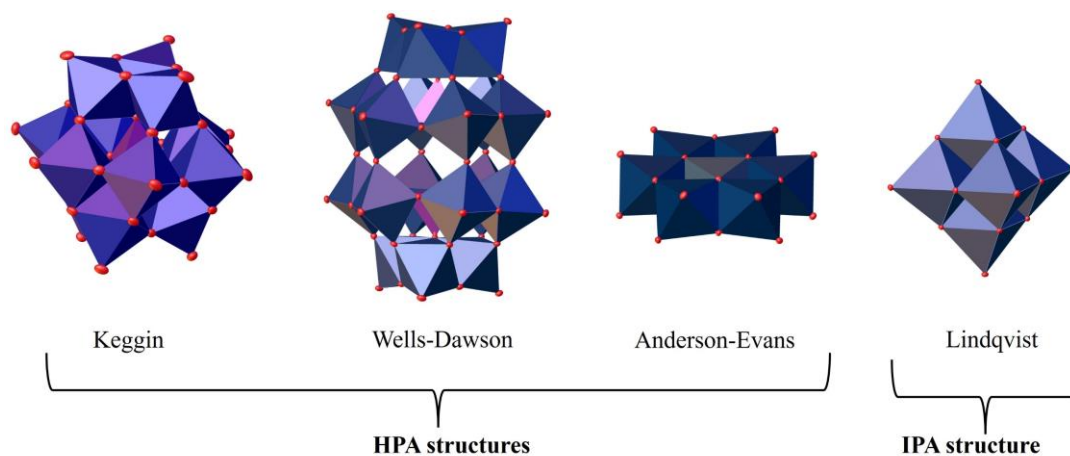


Figure S2: Structure types in POM chemistry. Keggin-, Wells-Dawson- and Anderson-type (HPA). Lindqvist-type (IPA).

Different positions of elements in a POM cluster, Figure S3:

- Heteroelement position (only in HPA structures)
- Ligand position (oxo ligands)
- Framework-element position (Mo, W)
- Foreign-element position (e. g. V)
- Cation position (H^+ , Na^+ , K^+ , NH_4^+ , organic cations)

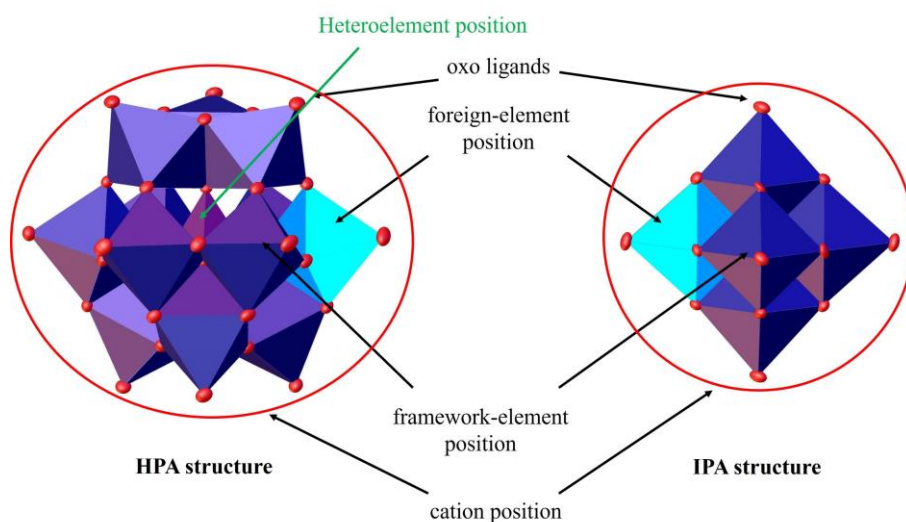


Figure S3: An element from the periodic table can occupy different positions in a POM cluster: the heteroelement position (only in HPA structures), the framework- or the foreign-element position, the cation and the ligand-position.

Solubility properties in dependence of the cation, Figure S4:

- Cations like H^+ , Na^+ , K^+ result in water-soluble materials
- Cations like Cs^+ result in insoluble materials
- Organic cations like tetrabutyl ammonium result in materials, that are soluble in organic solvents (e.g. acetonitrile)

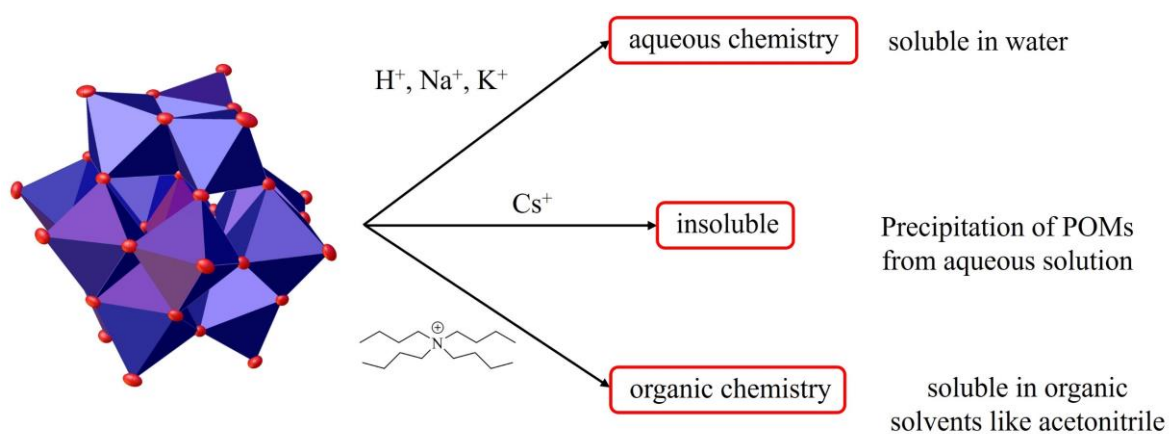


Figure S4: Solubility of POMs in different media by choosing the correct cation.

2 Experimental part

2.1 Chemicals

The chemicals used were purchased from the following suppliers:

- Sodium tungstate dihydrate: VWR chemicals ($\geq 99\%$ for analysis)
- Phosphoric acid: was purchased as a 85 % solution in water from Grüssing
- Acetic acid: 99 % VWR chemicals
- Tetrabutylammonium bromide (TBAB): Carl Roth with a purity of 99 %
- Orange gel: VWR chemicals
- Silver tungstate: 99 % abcr
- Acetonitrile: Sigma Aldrich, HPLC grade
- 37 % Hydrochloric acid solution in water: 37 % VWR chemicals
- Aluminium trichloride: Strem Chemicals
- Tetrahydrofurane (THF): Sigma Aldrich, Spectroscopic grade, distilled
- 2 M solution of hydrochloric acid in diethyl ether: Sigma Aldrich, Anhydrous
- Dichloromethane: FisherSci, HPLC grade
- Tetraethyl orthosilicate: Sigma Aldrich
- Potassium bromide: FisherSci
- Acetonitrile- d_3 : CIL, 99.5 % deuterated
- Benzyl bromide: Sigma Aldrich
- Ferrocene: Sigma Aldrich
- Tetrabutylammonium hexafluorophosphate: TCI, 95 %, recrystallized
- Silicotungstic acid hydrate: Sigma Aldrich

2.2 Experimental procedures

2.2.1 Synthesis of $\text{TBA}_9[\text{PW}_9\text{O}_{34}]$

Procedure adapted from Finke *et al.*^[1]

Sodium tungstate dihydrate (50.0043 g, 151.6 mmol, 5.9705 equivalents) was dissolved in deionized water (100 mL) and a 85 % solution of phosphoric acid in water (2.9455 g, 25.39 mmol, 1 equivalent) was added to the colourless solution. The pH value was 8.739. Acetic acid glacial (10.7064 g, 178.3 mmol, 7.022 equivalents) was added and the pH value changed to 6.954. It was stirred for two hours. Over night a colourless precipitate was formed, which was identified as $\text{Na}_9[\text{PW}_9\text{O}_{34}]$ (2.3419 g of a colourless solid) and was separated by filtration. A 0.407 M solution of tetrabutylammonium bromide in water (100 mL) was added and a colourless precipitate was formed, which was separated by filtration and was identified as $\text{TBA}_9[\text{PW}_9\text{O}_{34}]$. Both precipitates were dried in a desiccator under reduced pressure over orange gel for one night. A colourless powder (30.6439 g) was obtained.

ICP-OES: Calculated for $\text{TBA}_9[\text{PW}_9\text{O}_{34}]$: 37.504 % W, 0.702 % P, 0.00 % K, 0.00 % Na.

CHNS: Calculated for $\text{TBA}_9[\text{PW}_9\text{O}_{34}]$: 39.209 % C, 7.402 % H, 2.857 % N. **ICP-OES:** Found

for $\text{TBA}_9[\text{PW}_9\text{O}_{34}]$: 43.64 % W, 0.9042 % P, 0.00 % K, 0.07 % Na. **CHNS:** Found for

$\text{TBA}_9[\text{PW}_9\text{O}_{34}]$: 23.426 % C, 4.4694 % H, 1.708 % N. Data normalized to tungsten.

C/H/N/Na/K/P/W calculated: 144/324/9/0/0/1/9. Na/K/P/W found:

73.95/168.1/4.623/0.115/0.00/1.11/9. This corresponds to the stoichiometric formula

$(\text{TBA})_{4.623}\text{H}_{4.377}[\text{PW}_9\text{O}_{34}]$.

29.0008 g (12.6560 g W) of the powder was dried under reduced pressure in an oil bath, which was heated to 60 °C, over night. The dried powder was dissolved in dried acetonitrile (250 mL) in a volumetric flask. **$\text{TBA}_9[\text{PW}_9\text{O}_{34}]$ solution in acetonitrile.**

2.2.2 Synthesis of TBA_2WO_4

Procedure adapted according to Calmanti *et al.*^[2]

Tetrabutylammonium bromide (13.9079 g, 43.1 mmol 1.96 equivalents) was dissolved in water (50 mL). The solution was added to silver tungstate (10 g, 22 mmol, 1 equivalent) and the mixture was stirred for 90 minutes in the dark. It was filtered and the residue was washed three

times with water (50 mL). The water of the filtrate was evaporated under reduced pressure, yielding a yellow liquid (8.3 g).

ICP-OES: Calculated for TBA_2WO_4 : 25.089 % W, 0.00 % Ag. **CHNS:** Calculated for TBA_2WO_4 : 52.451 % C, 9.904 % H, 3.823 % N. **ICP-OES:** Found for TBA_2WO_4 : 22.20 % W, 0.0003 % Ag. **CHNS:** Found for TBA_2WO_4 : 46.71 % C, 9.775 % H, 3.135 % N. Data normalized to tungsten. C/H/N/Ag/W calculated: 32/72/2/0/1. C/H/N/Ag/W found: 32.20/80.31/1.85/2.45 · 10⁻⁵/1. This corresponds to the stoichiometric formula $(\text{TBA})_2[\text{WO}_4]$.

7.9559 g (1.7662 g) of the oil was dried under reduced pressure in an oil bath, which was heated to 60 °C, over night. The dried oil was dissolved in dried acetonitrile (50 mL) in a volumetric flask. **TBA₂WO₄ solution in acetonitrile.**

2.2.3 Synthesis of $\text{TBA}_3[\text{PW}_{12}\text{O}_{40}]$

$\text{TBA}_9[\text{PW}_9\text{O}_{34}]$ solution in acetonitrile (4.310 mL, 1.1869 mmol W, 3 equivalents) and TBA_2WO_4 solution in acetonitrile (2.059 mL, 0.3956 mmol 1 equivalent) were mixed and acidified with a 37 % hydrochloric acid solution in water (1 mL, 1.5830 mmol, 4 equivalents). A precipitate was formed and it was heated to 90 °C and stirred for one hour. After cooling to room temperature the precipitate was isolated by filtration and dried in a desiccator. A yellow powder (0.4401 g) was obtained.

ICP-OES: Calculated for $\text{TBA}_3[\text{PW}_{12}\text{O}_{40}]$: 61.205 % W, 0.859 % P. **CHNS:** Calculated for $\text{TBA}_3[\text{PW}_{12}\text{O}_{40}]$: 15.995 % C, 3.02 % H, 1.166 % N. **ICP-OES:** Found for $\text{TBA}_3[\text{PW}_{12}\text{O}_{40}]$: 55.9 % W, 0.813 % P. **CHNS:** Found for $\text{TBA}_3[\text{PW}_{12}\text{O}_{40}]$: 14.82 % C, 2.833 % H, 1.18 % N. Data normalized to tungsten. C/H/N/P/W calculated: 48/108/3/1/12. C/H/N/P/W found: 48.67/110.9/3.22/1.04/12.0. This corresponds to the stoichiometric formula $(\text{TBA})_3[\text{PW}_{12}\text{O}_{40}]$.

2.2.4 Synthesis of $\text{TBA}_6[\text{PAIW}_{11}\text{O}_{40}]$

$\text{TBA}_9[\text{PW}_9\text{O}_{34}]$ solution in acetonitrile (8.620 mL, 2.374 mmol W, 8.8417 equivalents) and an aluminium trichloride (0.0358 g, 0.2685 mmol, 1 equivalent) solution in THF (2 mL) were mixed. The colourless solution was acidified with a 2 M solution of hydrochloric acid in diethyl ether (2 mL, 4 mmol, 14.90 equivalents). After acidification, TBA_2WO_4 solution in acetonitrile (2.745 mL, 0.5275 mmol 1.9646 equivalents) was added and the solution was heated to 90 °C for one hour. After cooling to room temperature the solvent was removed under reduced pressure. The residue was dissolved in dichloromethane (10 mL) yielding a suspension with a

colourless solid, which was isolated by filtration and dried under reduced pressure. A colourless powder (0.4670 g) was obtained.

ICP-OES: Calculated for $\text{TBA}_6[\text{PAIW}_{11}\text{O}_{40}]$: 48.437 % W, 0.646 Al, 0.742 % P. **CHNS:** Calculated for $\text{TBA}_6[\text{PAIW}_{11}\text{O}_{40}]$: 27.618 % C, 5.215 % H, 2.013 % N. **ICP-OES:** Found for $\text{TBA}_6[\text{PAIW}_{11}\text{O}_{40}]$: 51.9 % W, 0.635 % Al, 0.87 % P. **CHNS:** Found for $\text{TBA}_6[\text{PAIW}_{11}\text{O}_{40}]$: 19.84 % C, 3.862 % H, 1.49 % N. Data normalized to tungsten. C/H/N/P/Al/W calculated: 96/216/6/1/1/11. C/H/N/P/Al/W found: 64.30/149.2/4.14/1.09/0.916/11.0. This corresponds to the stoichiometric formula $(\text{TBA})_4\text{H}_2[\text{PAIW}_{11}\text{O}_{40}]$.

2.2.5 Synthesis of $\text{TBA}_5[\text{PSiW}_{11}\text{O}_{40}]$

$\text{TBA}_9[\text{PW}_9\text{O}_{34}]$ solution in acetonitrile (2.845 mL, 0.7834 mmol W, 9.0150 equivalents) and a tetraethyl orthosilicate (0.0181 g, 0.0869 mmol, 1 equivalent) solution in THF (2 mL) were mixed. The colourless solution was acidified with a 2 M solution of hydrochloric acid in diethyl ether (1 mL, 2 mmol, 23.01 equivalents). After acidification, TBA_2WO_4 solution in acetonitrile (0.906 mL, 0.1741 mmol 2.0035 equivalents) was added and the solution was heated to 90 °C for 30 minutes. After cooling to room temperature water (10 mL) was added and a yellow precipitate was formed, which was isolated by filtration and dried under reduced pressure. A yellow powder (0.2160 g) was obtained.

The product seems to be soluble in dichloromethane.

ICP-OES: Calculated for $\text{TBA}_6[\text{PSiW}_{11}\text{O}_{40}]$: 51.409 % W, 0.714 Si, 0.787 % P. **CHNS:** Calculated for $\text{TBA}_6[\text{PSiW}_{11}\text{O}_{40}]$: 24.427 % C, 4.612 % H, 1.78 % N. **ICP-OES:** Found for $\text{TBA}_6[\text{PSiW}_{11}\text{O}_{40}]$: 56.1 % W, 0.638 % Si, 0.80 % P. **CHNS:** Found for $\text{TBA}_6[\text{PSiW}_{11}\text{O}_{40}]$: 17.98 % C, 3.472 % H, 1.32 % N. Data normalized to tungsten. C/H/N/P/Si/W calculated: 80/180/5/1/1/11. C/H/N/P/Si/W found: 53.93/124.1/3.40/0.927/0.818/11.0. This corresponds to the stoichiometric formula $(\text{TBA})_{3.37}\text{H}_{1.63}[\text{PSiW}_{11}\text{O}_{40}]$.

2.2.6 Reactivity study

A 77 mmol solution of benzyl bromide in acetonitrile- d_3 (76 μL , 5.9 μmol , 1.16 equivalents) was added to the POM (5.08 μmol , 1 equivalent) and heated to 60 °C for one hour. After cooling to room temperature, the NMR measurements were performed (^1H , ^{13}C and ^{31}P).

POM nBu₄NPW: 0.0183 g

POM nBu₄NPAIW: 0.0194 g

2.3 Characterization

2.3.1 Compositional analysis

Elemental analysis:

a) Inductively coupled plasma optical emission spectroscopy (ICP-OES) and flame atomic absorption spectroscopy (F-AAS):

All samples were analyzed using an ICP-OES-spectrometer for elemental analysis (Fa. Spectro, type ARCOS) for W, Al, Si and P (method ICP-OES). Na, K and Ag were determined with AAS-F (Fa. Thermo, type Solaar S Series), method: F-AAS without HKL.

- Compound $\text{TBA}_9[\text{PW}_9\text{O}_{34}]$ and TBA_2WO_4 were digested with a microwave digestion: weight + 5 mL aqua regia (inverse) + 1 mL of hydrofluoric acid. The solution was filled up with water in a 15 mL volumetric flask.
- Compound $\text{TBA}_3[\text{PW}_{12}\text{O}_{40}]$ was digested with a microwave digestion: weight + 5 mL aqua regia (inverse) + 1 mL of hydrofluoric acid in the microwave at 250 °C. The solution was filled up with water in a 15 mL volumetric flask.
- Compound $\text{TBA}_6[\text{PAIW}_{11}\text{O}_{40}]$ was digested with a microwave digestion: weight + 5 mL aqua regia (inverse) in the microwave at 250 °C. The solution was filled up with water in a 15 mL volumetric flask.
- Compound $\text{TBA}_5[\text{PSiW}_{11}\text{O}_{40}]$ was digested with a melt digestion: weight + lithium metaborate + sodium/potassium carbonate (150/150 mg) + 5 mL 8 % nitric acid in water. The solution was filled up with water in a 50 mL volumetric flask.

b) CHNS analysis

- Compound TBA_2WO_4 was measured with a "Unicube" of the company "Elementar".
- Compound $\text{TBA}_3[\text{PW}_{12}\text{O}_{40}]$, $\text{TBA}_6[\text{PAIW}_{11}\text{O}_{40}]$ and $\text{TBA}_5[\text{PSiW}_{11}\text{O}_{40}]$ were measured with a "Unicube" of the company "Elementar".

Results from the elemental analysis are shown in Table S1.

Tab. S1: Results from elemental analysis for the Al and Si substituted Keggin-type structures. The stoichiometric ratios were verified by ICP-OES (P, Al, Si, W) and CHNS (C, H, N).

POM	Observed stoichiometry	C	H	N	P	Al	Si	W
nBu₄NPW	3 (C ₁₆ H ₃₆ N) ⁺ [PW ₁₂ O ₄₀] ³⁻	48.67	110.9	3.22	1.04	-	-	12.0
nBu₄NPAIW	4 (C ₁₆ H ₃₆ N) ⁺ 2 H ⁺ [P _{1.1} Al _{0.92} W ₁₁ O ₄₀] ⁶⁻	64.30	149.2	4.14	1.09	0.916	-	11.0
nBu₄NPSiW	3.37 (C ₁₆ H ₃₆ N) ⁺ 1.63 H ⁺ [P _{0.93} Si _{0.82} W ₁₁ O ₄₀] ⁵⁻	53.93	124.1	3.40	0.927	-	0.818	11.0

2.3.2 Vibrational Spectroscopy

Infrared (IR) spectroscopy:

Infrared spectra were obtained on a Thermo Scientific Nicolet NXR 9650 FT-Infrared Spectrometer instrument equipped with a 1064 nm Nd:YVO₄ laser and InGaAs detector, on KBr plates or as a KBr pellet.

The data were exported as .dpt file and plotted in Origin2019b.

Raman spectroscopy:

The Raman spectra of the compounds were measured on a SENTERRA Raman microscope from Bruker Optik GmbH. Here, the aperture was set to 50 x 1000 μm and a 20 objective was used on the microscope. The excitation laser had a wavelength of 785 nm and the measurement range was between 75 cm^{-1} and 1525 cm^{-1} . An integration time of 16 seconds was used, the number of scans was 8 and the Raman laser power was 10 mW. All data were exported as .dpt file and plotted in Origin®2019b.

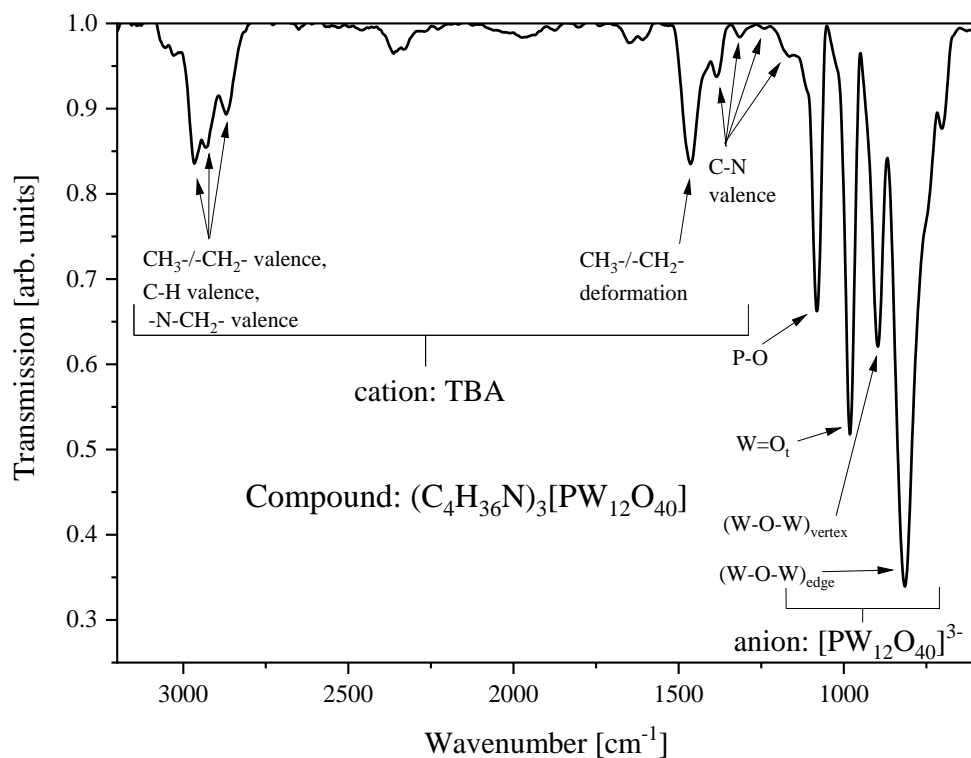


Figure S5: IR spectrum (KBr) of compound **nBu₄NPW**. All vibrational bands for the cations are found above 1200 cm⁻¹ and the bands of the anion are in the range of 1200 to 600 cm⁻¹.^[3,4]

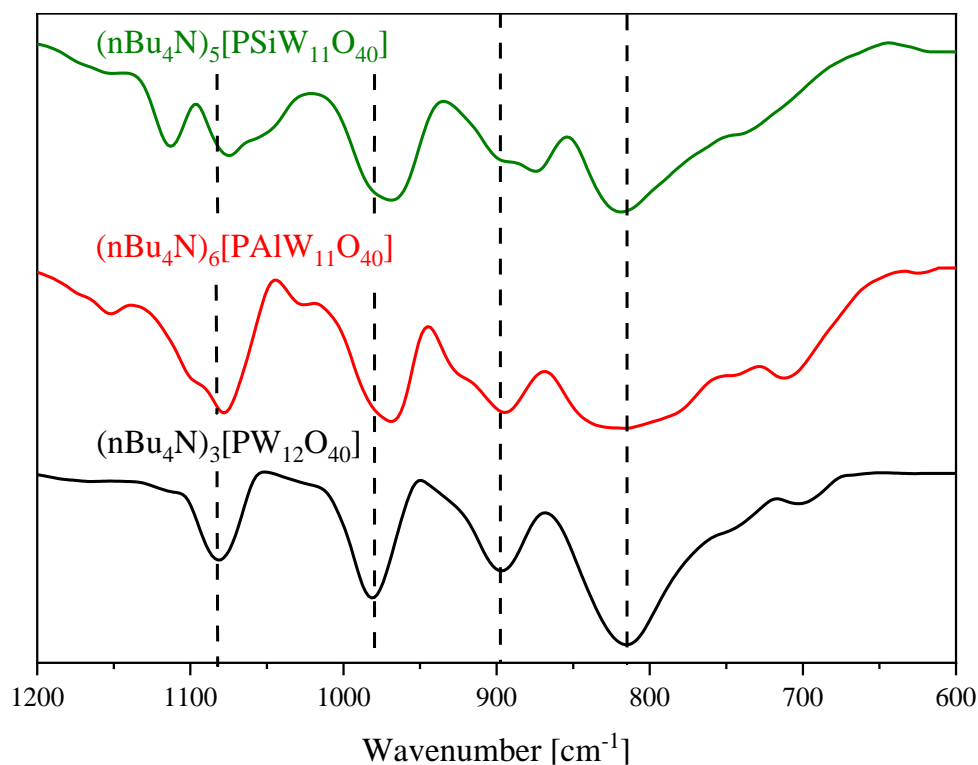


Figure S6: IR spectra (KBr) of compounds **PW**, **PAIW** and **PSiW**.

In Figure S5 the IR spectrum of the Keggin-type compound **nBu₄NPW** is shown. All vibrational modes, that are relevant for identifying the structure-type, are found on the right side in the range between 1200 to 600 cm^{-1} . Vibrational modes above 1200 cm^{-1} belong to the vibrational bands of the TBA cation. Here, the P-O vibrational band is found at 1082 cm^{-1} , the M=O_t (vibrations of terminal oxygen atoms) at 981.7 cm^{-1} and the different types of M-O-M modes are found at 897 and 816 cm^{-1} .^[3,4] Since the vibrational bands for cations and anions are separated in the IR spectra, an interpretation is easy. Therefore, only the vibrational bands in the range between 1200 and 600 cm^{-1} are relevant for evaluating the success of the experiments (Figure S6).

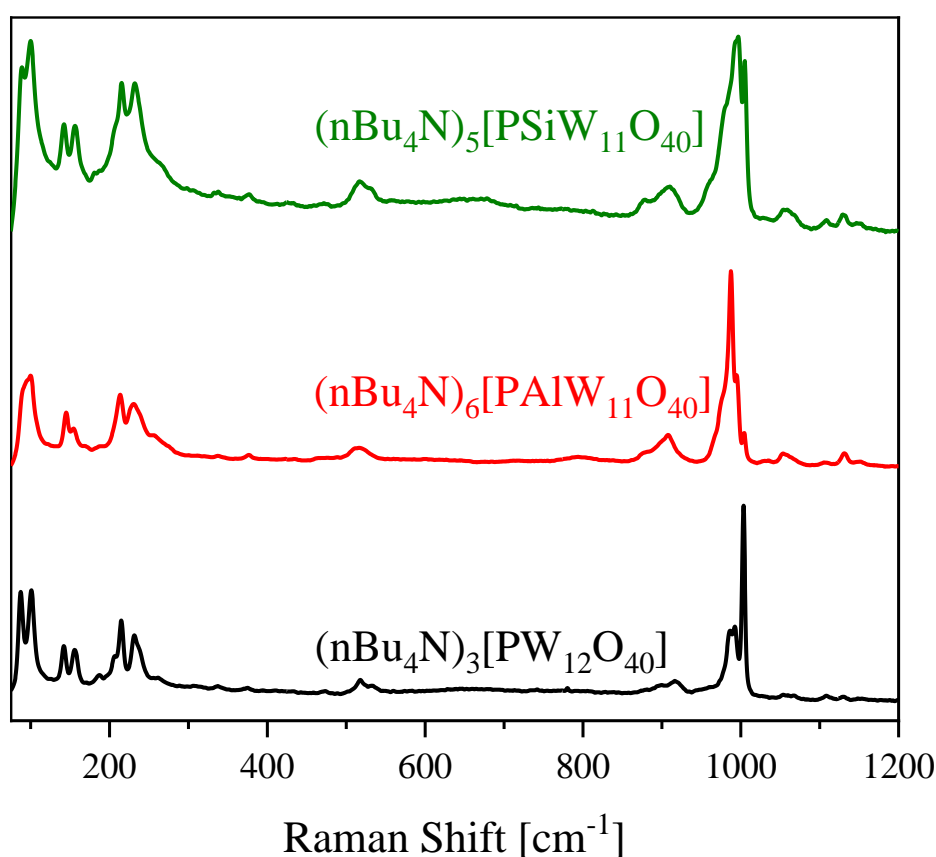


Figure S7: Raman spectra of compounds **PW**, **PAIW** and **PSiW**.

The synthesis success for the foreign-element substitution is indicated by the P-O band for compound **nBu₄NPSiW** splitting into two separate bands, while for both compounds, **nBu₄NPSiW** and **nBu₄NPAIW**, the bands become broader and shift to lower wavenumbers. All effects described here can be explained by the large mass difference between W and Si or Al. Since the Si and Al substitutional elements are significantly lighter than W, the associated vibrational bands are easier to excite. A lower excitation energy correlates with a lower

wavenumber, which also explains the shoulder formation. The broadened vibrational bands for M-O-M could be interpreted as a superposition of the modes Al/Si-O-W and W-O-W.

The success of the element substitution becomes clear from the Raman spectra as the $M=O_t$ vibrational modes (in the range 950 to 1000 cm^{-1}) change in their shape and position. A broadening of the bands is also recognizable here, which could be explained by a superposition of the Al/Si= O_t and W= O_t vibrational bands.

IR spectra of **PSiW** (left) and commercial available $H_4[SiW_{12}O_{40}]$ (right) in Figure S8:

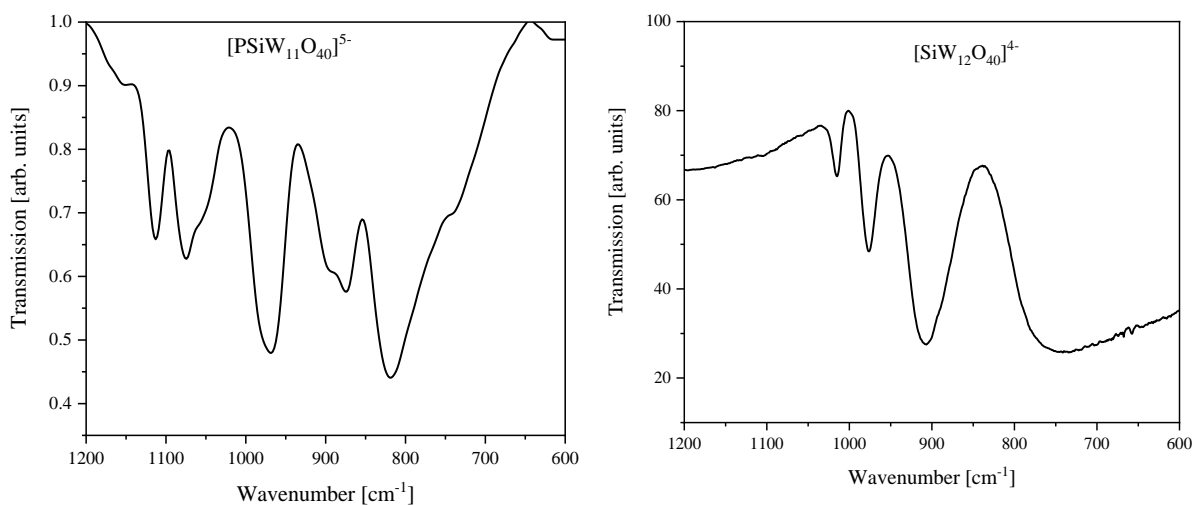


Figure S8: IR spectra of **PSiW** and $H_4[SiW_{12}O_{40}]$.

2.3.3 Crystallography

Single-crystal X-ray diffraction (sc-XRD):

The single crystals discussed here were measured on a single-crystal diffractometer with four circles: SuperNova Oxford Diffraction from Agilent Technologies.

- Equipped with a molybdenum and copper source as a dual instrument with microfocus tubes
- Cryostream-700 Plus nitrogen flow cooling, 100-500 K (Oxford Cryosystems)

All data were refined with the Software Olex2 v1.5, the ShelX algorithm and the software PLATON. For verification of the space group the tool XPREP of the software Shelxtl was used.^[5-9] The final crystallographic data were saved as .cif file and were checked with the publication online tool CheckCIF <https://checkcif.iucr.org/>.^[10]

The .cif files were published in the Cambridge Crystallographic Data Centre and Fachinformationszentrum Karlsruhe Access Structures service database with the deposition number 2441126: <https://www.ccdc.cam.ac.uk/>.

Crystallographic Discussion

The phosphorus atom is the center of a disorder. Here, the phosphorus atom appears in a cubic coordination geometry of eight oxygen atoms. The solid-state structure consists of two Keggin-type species in which the PO₄ tetrahedra are rotated by 90 ° to each other (inversion of the asymmetric unit (AU) at P1). Therefore, a non-positive definite (NPD) was obtained. The displacement parameters were therefore set to a reasonable positive value using constraints.

For example, NPDs can appear, if the atom type was wrongly assigned. To exclude this we refined the AU of the model with other atom types in the position of the heteroelement that can be found in our new compound (oxygen, tungsten and aluminium). The results are shown in Figure S9 and show that the model has been significantly worsed (note: it is not possible to distinguish phosphorus from aluminium by crystallography).

From a chemical point of view, an exchange of the heteroelement during the POM synthesis can be excluded, since the POM was synthesized from the tungsten-based Lacunary-type structure [PW₉O₃₄]⁹⁻, which already carries the heteroelement phosphorus. The chemical reaction to incorporate the foreign-element takes place in the framework element position and leaves the heteroelement untouched. Oxygen and tungsten can be excluded as heteroelements,

as the heteroelement is in a tetrahedral coordination environment of four oxygen atoms and peroxide formation can be excluded in this way. Due to the enormous ionic size, only octahedral oxygen compounds are known for tungsten. Only an exchange by aluminium would be conceivable. However, it was still possible to detect the phosphorus in the desired stoichiometry using elemental analysis. Therefore, an assignment of the wrong element can be ruled out in this case.

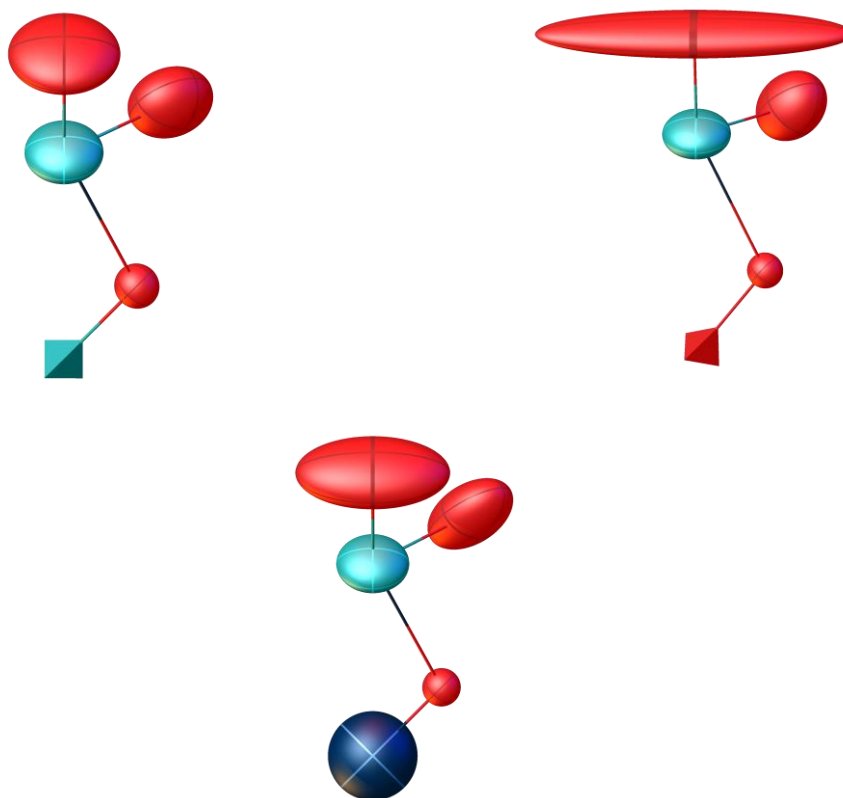


Figure S9: Refinement results of the heteroelement atom type assignment of the AU (aluminium - turquoise top left, oxygen - red top right and tungsten - blue bottom). The following crystallographic quality parameters were found: 1. aluminium (top left) R_1 : 4.92 %, wR_2 : 12.38 %, R_{int} : 9.58 % and GooF: 1.070. 2. oxygen (top right) R_1 : 11.24 %, wR_2 : 35.62 %, R_{int} : 9.58 % and GooF: 1.186. 3. tungsten (bottom) R_1 : 13.33 %, wR_2 : 46.24 %, R_{int} : 9.58 % and GooF: 2.052.

Powder X-ray diffraction

pXRD data of all investigated POMs are shown in Figure S10:

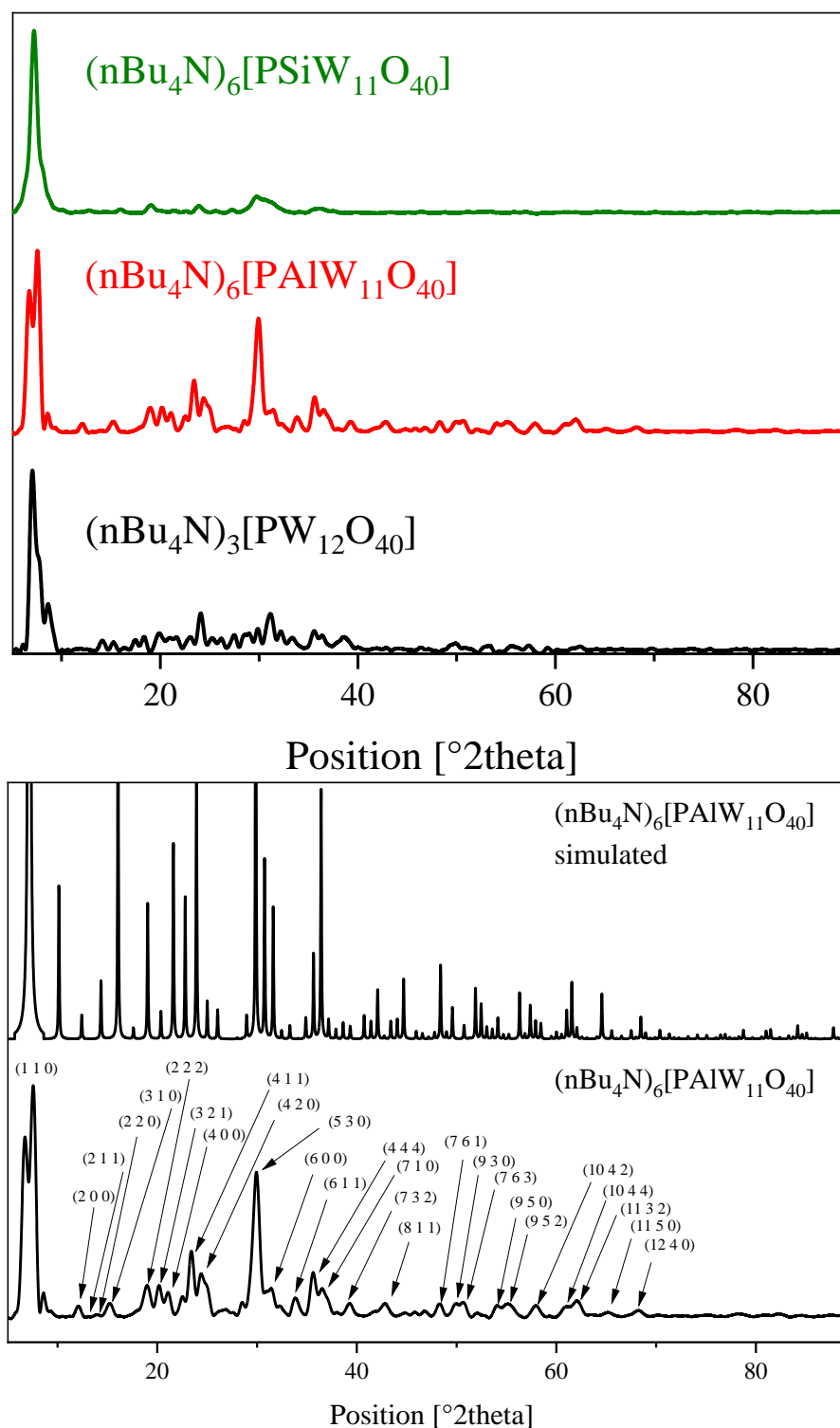


Figure S10: Top: pXRD data of all investigated POMs in the angle range 5 to 90 $^{\circ}$. Bottom: Measured pXRD of compound $n\text{Bu}_4\text{NPAIW}$ in comparison with the in Mercury simulated pXRD (.cif file). Assumed wavelength of the X-ray radiation: 1.54056 \AA . The assignment of the Miller indices to the measured reflexes is based on the simulated data.

It is difficult to interpret the pXRD data, as POMs are usually not phase-pure, but a mixture of various solid-state phases. This observation is consistent with our previous observations.^[11–14] An assignment of Miller's indices to the measured reflections is based on a simulation of the pXRD data from the scXRD data of the compound **nBu₄NPAIW**. The reflexes (1 1 0), (4 1 1) and (5 3 0) are particularly intense here. The reflex (1 1 0) appears to be present twice, once at 7.55 ° and 6.72 °. So, compound **nBu₄NPAIW** is present at least in the form of two solid-state phases, while one solid-state phase was preferentially isolated by the crystallization of the POM.

Bond length discussion

Bond lengths of anion **PAIW** in comparison with the sum of covalent radii, Table S2.^[15]

Tab. S2: Bond lengths of the anion **PAIW** in comparison with the sum of covalent radii.^[15]

Bond type	Found bond length [Å]	Sum of covalent radii ^[15] [Å]	Literature values [PW ₁₂ O ₄₀] ³⁻ deposition number: 788692 ^[16]
P ₁ -O ₁	1.537	1.74	1.530
O ₁ -M ₁	2.437	1.99*	2.476
M ₁ -O ₂	1.864	1.99*	1.883
M ₁ =O ₃	1.674	1.99*	1.664

*values were calculated as weighted sum of covalent radii with the radii r and the weighing factors a ($= 1$) and b ($= 11$)

$$r_w = \frac{a(r_{Al} + r_O) + b(r_W + r_O)}{a + b}$$

The TBA cations are so strong disordered, that a solvent-mask (aka SQUEEZE) was used and the void was assigned to the TBA cations. Here, the POM anion was crystallized in the cubic space group Im-3m (229) and was identified with a disorder of the central PO₄ tetrahedron. The four oxygen atoms of the PO₄ tetrahedron are displaced from each other by 90 °, which means that the central phosphorus atom is surrounded by eight oxygen atoms in a cube shape. To model this disorder the occupancy factors of the eight oxygen atoms were refined to 0.5. In this solid-state structure, the asymmetric unit contains five atoms, one phosphorous, three oxygen and one metal atom. No concrete substitution pattern was observed, because the Al atom is statistically distributed over all twelve metal positions. Here, using the exyz command, the occupancy of the metal atom was refined with 1/12 to Al and 11/12 to W, resulting in a significant reduction of the R_1 value. As already shown in a previous study on tungsten clusters,

similar problems were encountered in treating the absorption effect of heavy atoms, resulting in a residual electron density with a maximum and minimum peak of 1.2 and -1.9.^[17]

2.3.4 NMR Spectroscopy

Nuclear magnetic resonance spectra were collected on either a Bruker AV 400 spectrometer or a Bruker AV 500 MHz spectrometer equipped with a cryoprobe. All NMR spectra are referenced to tetramethylsilane (^1H , ^{13}C), H_3PO_4 (^{31}P), and CFCl_3 (^{19}F).

^{27}Al NMR spectra were measured on a Bruker AVANCE III HD 400 MHz spectrometer (AVIII400) with a base frequency of 400 MHz. The spectra were referenced to $\text{Al}(\text{NO}_3)_3$.

- 5 mm BBFO sample head (Smart Probe) with ATM and z-gradientxviii
- Sample changer: SampleXpress Lite (16 samples)
- TOPSPIN 3.6.4

The data evaluation was done in MestReNova® and all data were exported as .csv file and plotted in Origin2019b.

The unsubstituted Keggin species $[\text{PW}_{12}\text{O}_{40}]^{3-}$ was identified at a chemical shift of -15.3 ppm. Peaks at -12.9 and 13.3 ppm can be assigned to the species $[\text{PAIW}_{11}\text{O}_{40}]^{6-}$ and $[\text{PSiW}_{11}\text{O}_{40}]^{5-}$. In general, Si and Al have fewer electrons than W, which explains the shift of the ^{31}P signals to higher ppm values. In the spectra of the Al- and Si-substituted POMs, peaks at -15.3 ppm were also found, which can be assigned to the unsubstituted species $[\text{PW}_{12}\text{O}_{40}]^{3-}$. According to the integrals, the two species were present in a ratio of 9.30 to 1 (**PAIW/PW**) and 2.84 to 1 (**PSiW/PW**). This could be interpreted as a hint for dissociation equilibria of POMs in acetonitrile solution. POM dissociations have already been discussed in detail for aqueous media.^[13,18] However, a dissociation can be excluded for POMs in completely dry organic media, since the POMs with TBA cations have no protons available that could initiate a dissociation of the clusters. But since the POMs were prepared in acidic acetonitrile solution, it is possible that not every cation position is occupied by TBA cations. The cation positions could also be partially filled with protons, resulting in compounds of the general types $\text{TBA}_{6-x}\text{H}_x[\text{PAIW}_{11}\text{O}_{40}]$. These protons could dissociate in acetonitrile solution and catalyze the dissociation of the POM clusters. The dissociations of POMs in solution are generally reversible equilibria, whereby the equilibrium is always on the side of the intact POM, if the solvent is removed.^[13] This hypothesis is strengthened by the missing C/H/N contents detected by CHNS analysis (Table 1, main manuscript), which suggests that additional protons are present and

responsible for the dissociations of the substituted anions. Since the precursors were not produced in completely dry solvents, the presence of a small amount of water would also be conceivable, which would initiate the dissociation.

Dissociation would also be conceivable in anhydrous solutions containing acetonitrile, where individual M=O fragments would be released from the POM cluster as $[O=M(NCCH_3)_n]$.

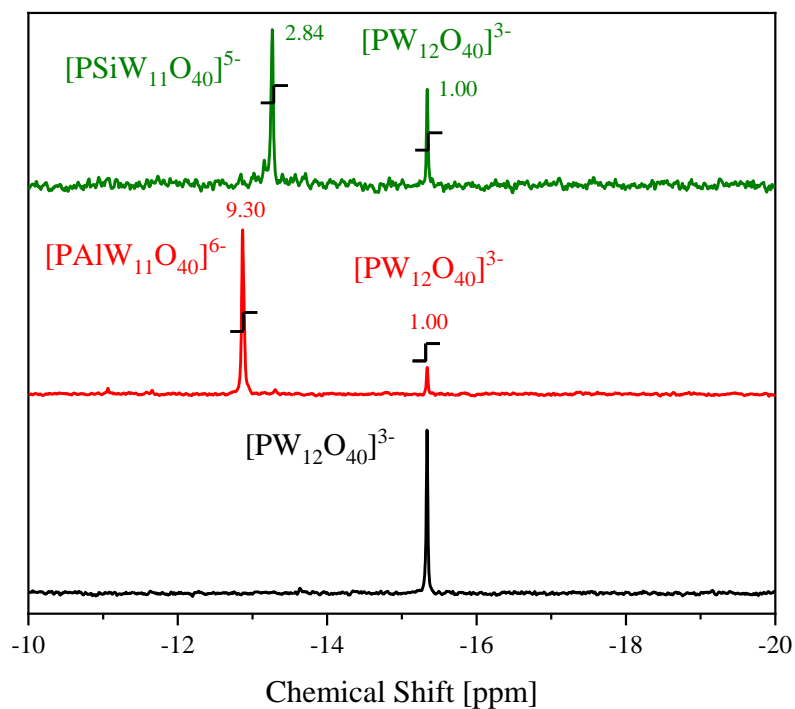


Figure S11: ^{31}P -NMR spectra of the investigated POMs, measured in acetonitrile- d_3 solution. The spectra were measured at a frequency of 161.9 MHz, with aqueous H_3PO_4 solution as reference (0 ppm).

^1H NMR (400 MHz) of compound $\text{TBA}_3[\text{PW}_{12}\text{O}_{40}]$ in acetonitrile- d_3 (Figure S12):

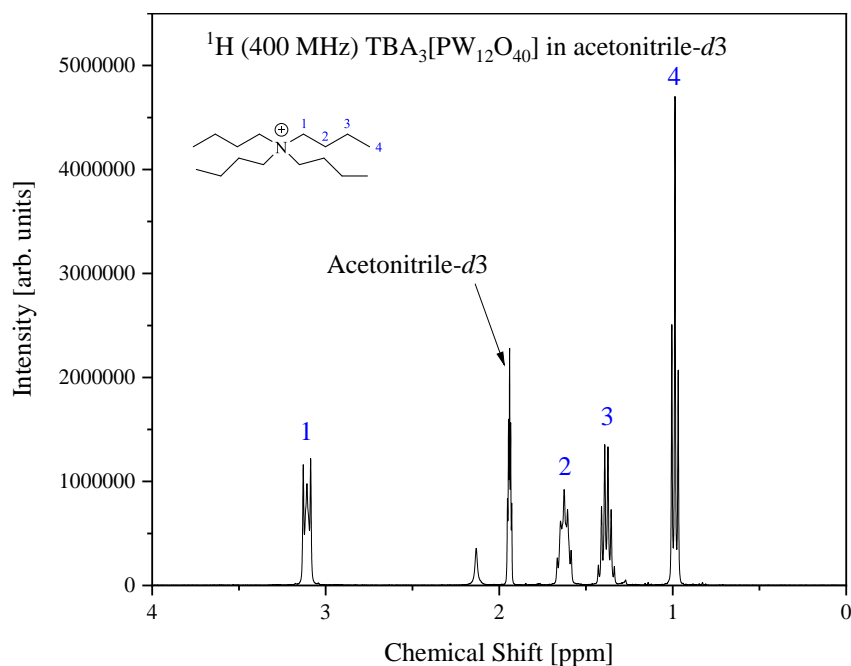


Figure S12: ^1H NMR of compound $\text{TBA}_3[\text{PW}_{12}\text{O}_{40}]$. The spectrum was measured at 400 MHz using tetramethyl silane in chloroform as reference (0 ppm).

^{13}C NMR (100 MHz) of compound $\text{TBA}_3[\text{PW}_{12}\text{O}_{40}]$ in acetonitrile- d_3 (Figure S13):

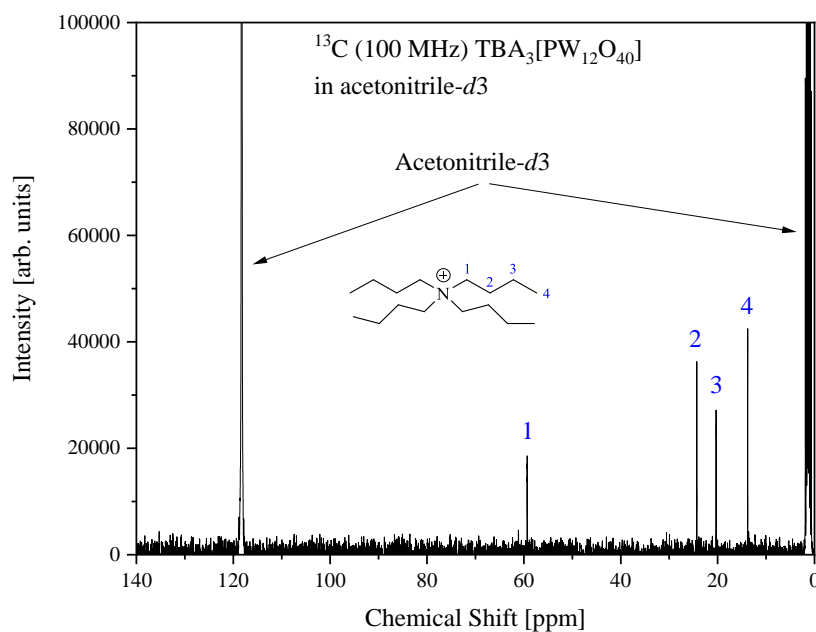


Figure S13: ^{13}C NMR of compound $\text{TBA}_3[\text{PW}_{12}\text{O}_{40}]$. The spectrum was measured at 100 MHz using tetramethyl silane in chloroform as reference (0 ppm).

^{13}C -DEPTQ NMR (100 MHz) of compound $\text{TBA}_3[\text{PW}_{12}\text{O}_{40}]$ in acetonitrile- d_3 (Figure S14):

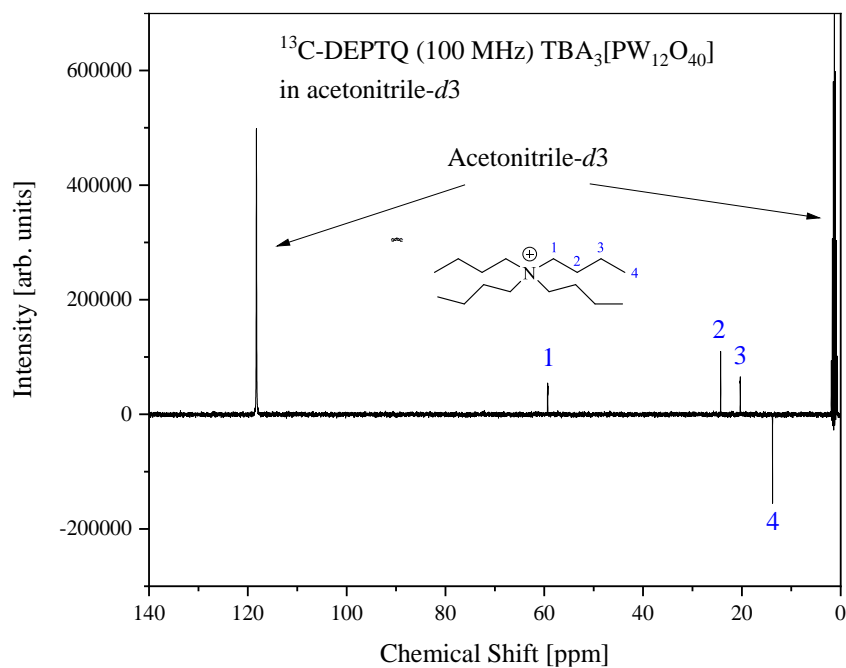


Figure S14: ^{13}C -DEPTQ NMR of compound $\text{TBA}_3[\text{PW}_{12}\text{O}_{40}]$. The spectrum was measured at 100 MHz using tetramethyl silane in chloroform as reference (0 ppm).

^1H NMR (400 MHz) of compound $\text{TBA}_6[\text{PAIW}_{11}\text{O}_{40}]$ in acetonitrile- d_3 (Figure S15):

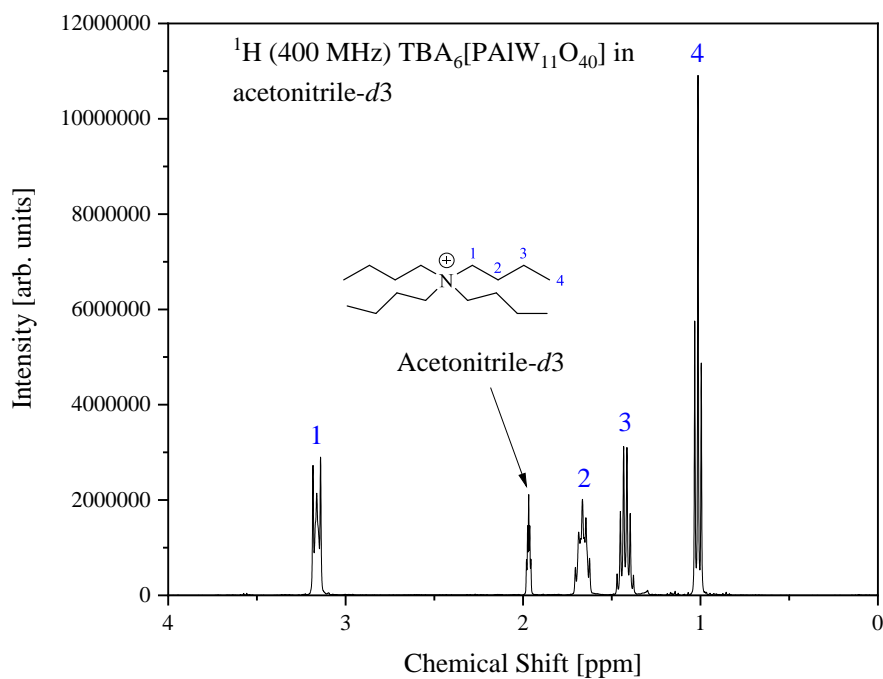


Figure S15: ^1H NMR of compound $\text{TBA}_6[\text{PAIW}_{11}\text{O}_{40}]$. The spectrum was measured at 400 MHz using tetramethyl silane in chloroform as reference (0 ppm).

^{13}C NMR (100 MHz) of compound $\text{TBA}_6[\text{PAIW}_{11}\text{O}_{40}]$ in acetonitrile- d_3 (Figure S16):

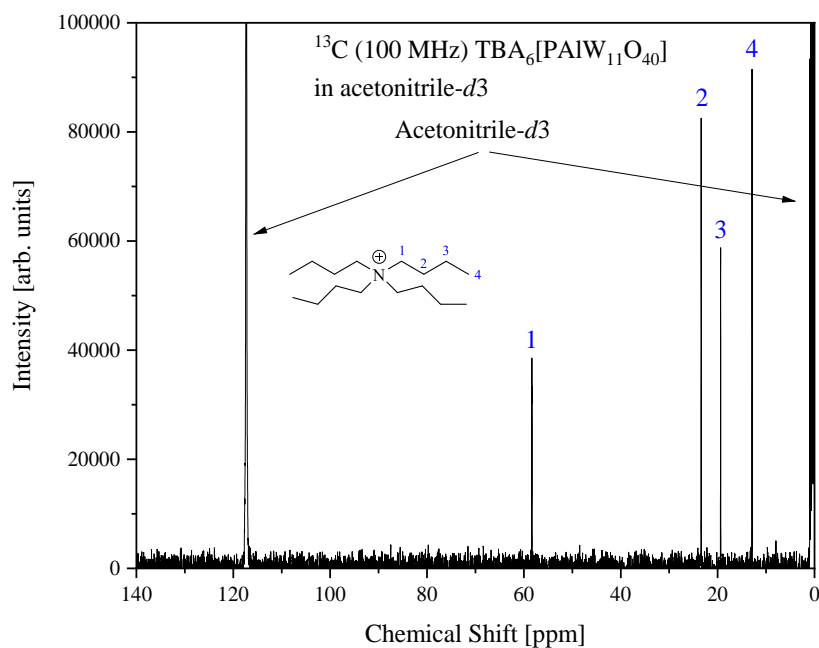


Figure S16: ^{13}C NMR of compound $\text{TBA}_6[\text{PAIW}_{11}\text{O}_{40}]$. The spectrum was measured at 100 MHz using tetramethyl silane in chloroform as reference (0 ppm).

^{13}C -DEPTQ NMR (100 MHz) of compound $\text{TBA}_6[\text{PAIW}_{11}\text{O}_{40}]$ in acetonitrile- d_3 (Figure S17):

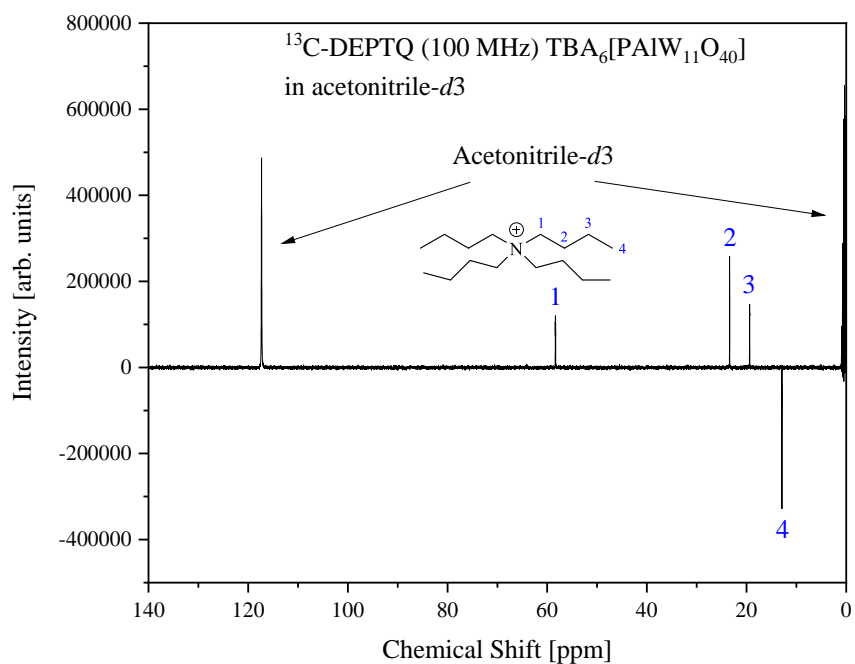


Figure S17: ¹³C-DEPTQ NMR of compound TBA₆[PAIW₁₁O₄₀]. The spectrum was measured at 100 MHz using tetramethyl silane in chloroform as reference (0 ppm).

¹H NMR (400 MHz) of compound TBA₅[PSiW₁₁O₄₀] in acetonitrile-*d*₃ (Figure S18):

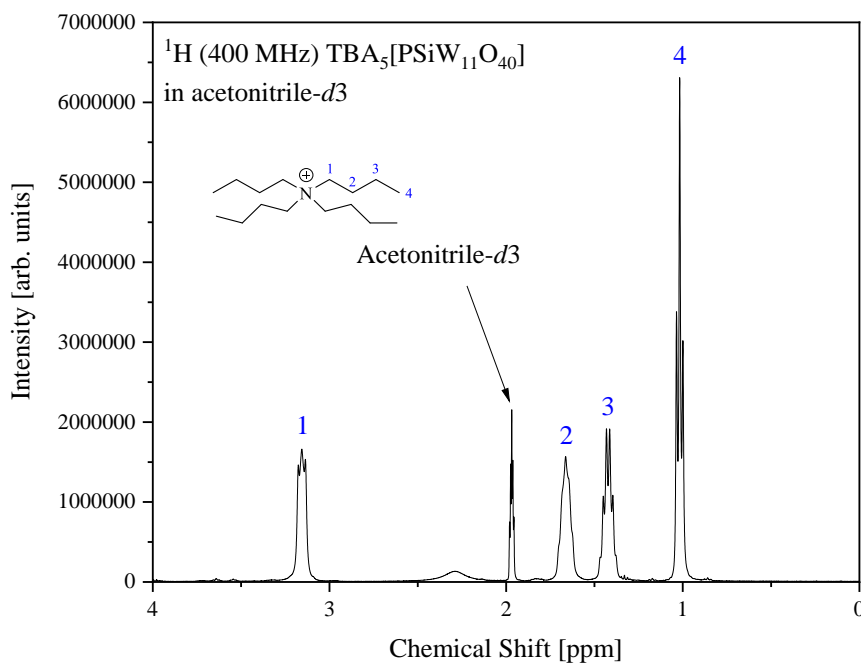


Figure S18: ¹H NMR of compound TBA₅[PSiW₁₁O₄₀]. The spectrum was measured at 400 MHz using tetramethyl silane in chloroform as reference (0 ppm).

¹³C NMR (100 MHz) of compound TBA₅[PSiW₁₁O₄₀] in acetonitrile-*d*₃ (Figure S19):

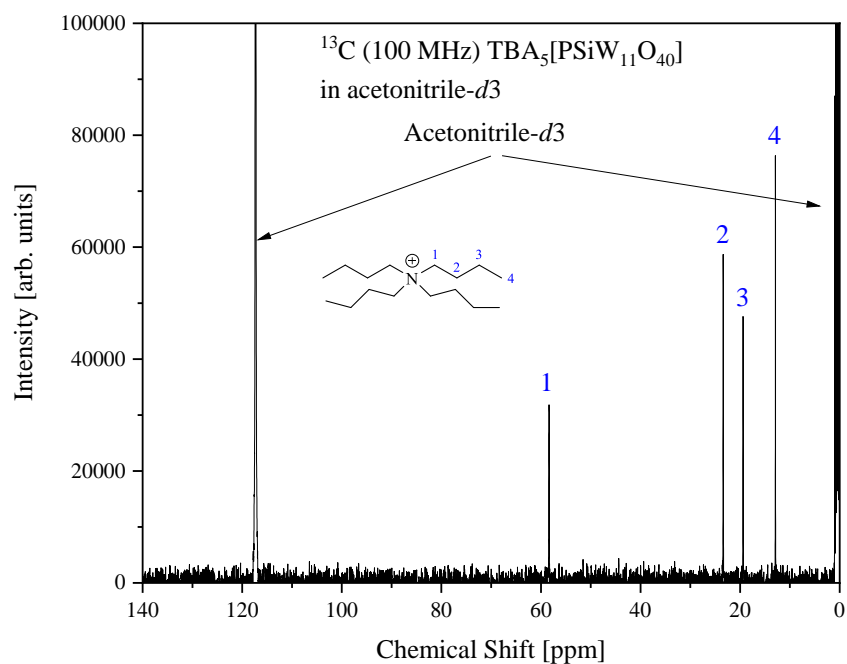


Figure S19: ^{13}C NMR of compound $\text{TBA}_5[\text{PSiW}_{11}\text{O}_{40}]$. The spectrum was measured at 100 MHz using tetramethyl silane in chloroform as reference (0 ppm).

^{13}C -DEPTQ NMR (100 MHz) of compound $\text{TBA}_5[\text{PSiW}_{11}\text{O}_{40}]$ in acetonitrile- d_3 (Figure S20):

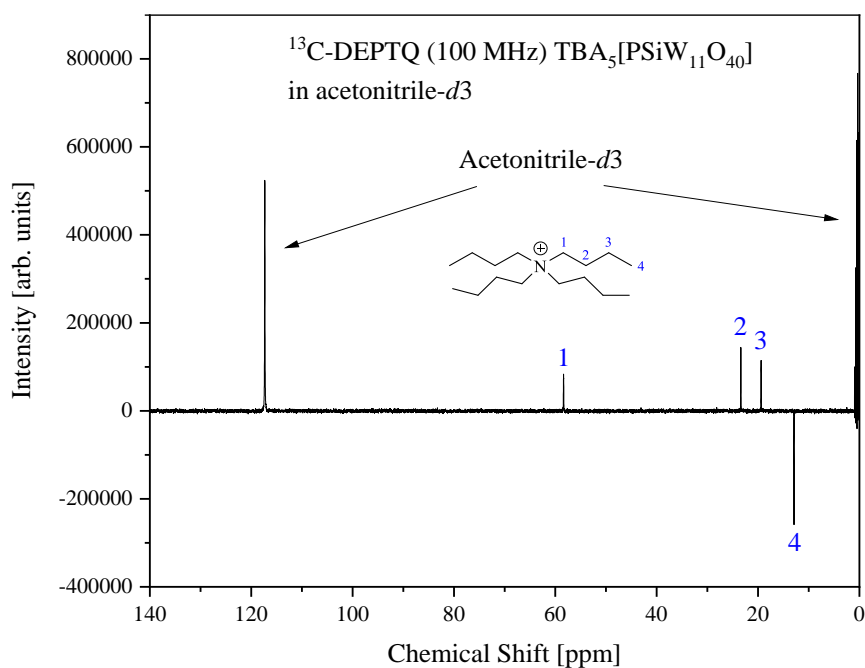


Figure S20: ^{13}C -DEPTQ NMR of compound $\text{TBA}_5[\text{PSiW}_{11}\text{O}_{40}]$. The spectrum was measured at 100 MHz using tetramethyl silane in chloroform as reference (0 ppm).

^1H NMR (400 MHz) of benzyl bromide in acetonitrile- d_3 (Figure S21):

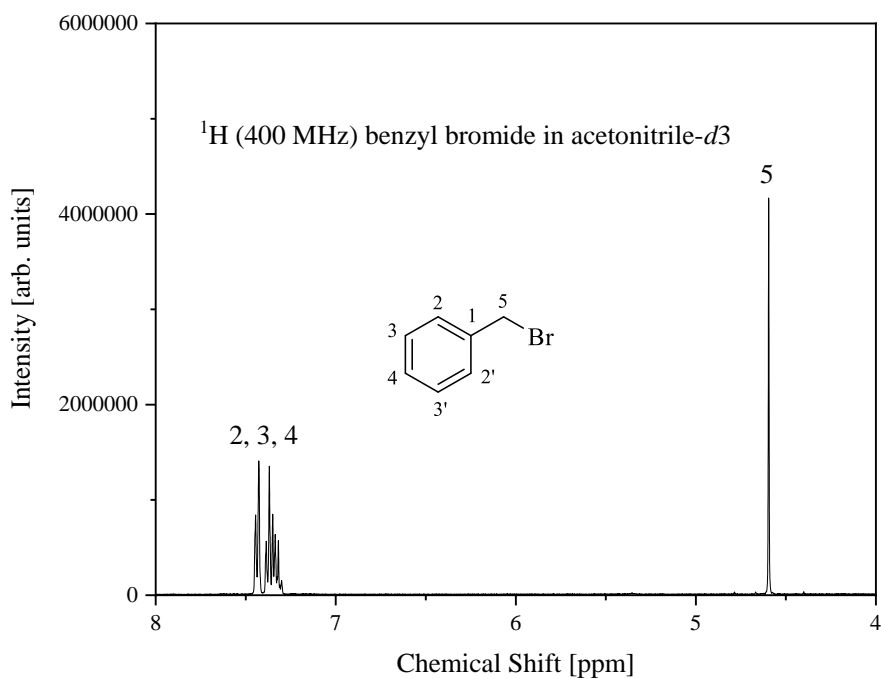


Figure S21: ¹H NMR of benzyl bromide in acetonitrile-*d*3. The spectrum was measured at 400 MHz using tetramethyl silane in chloroform as reference (0 ppm).

¹³C NMR (400 MHz) of benzyl bromide in acetonitrile-*d*3 (Figure S22):

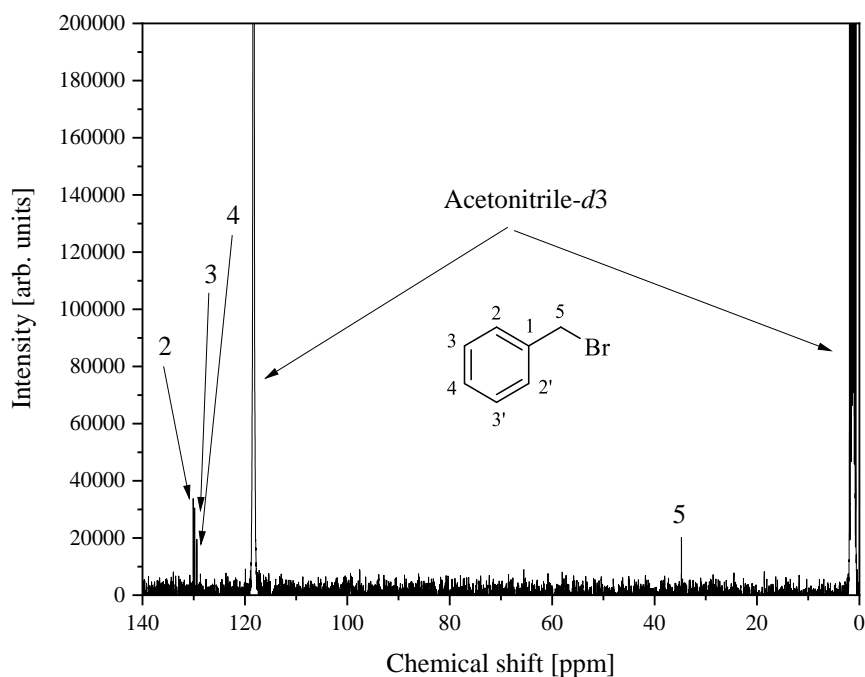


Figure S22: ¹³C NMR of benzyl bromide in acetonitrile-*d*3. The spectrum was measured at 100 MHz using tetramethyl silane in chloroform as reference (0 ppm).

¹H NMR (400 MHz) reactivity study in acetonitrile-*d*3 (Figure S23):

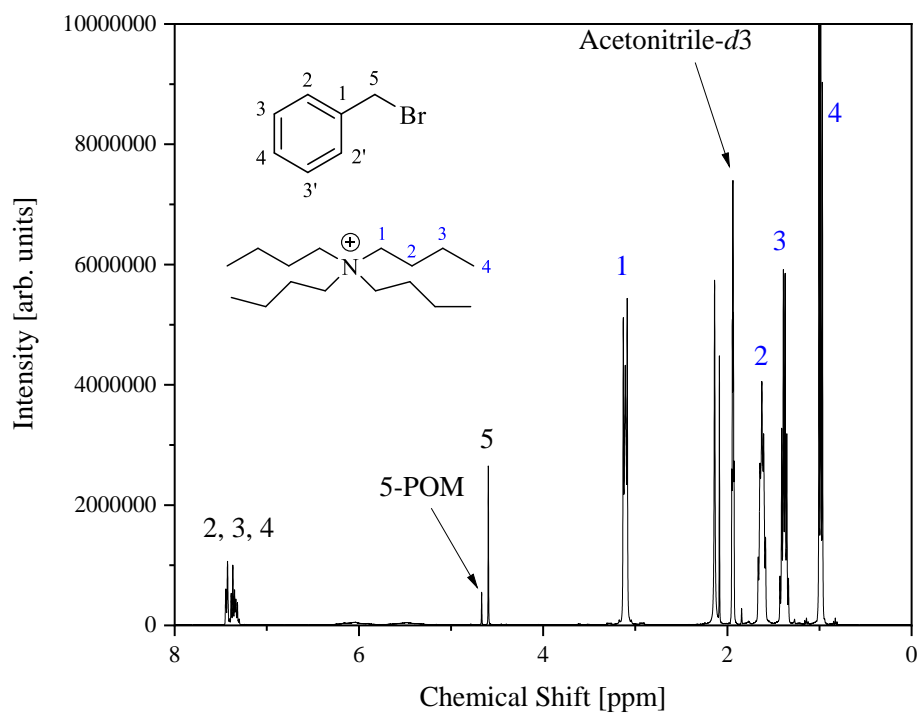


Figure S23: ^1H NMR of benzyl bromide and POM $n\text{Bu}_4\text{NPW}$ in acetonitrile- d_3 (reactivity study). The spectrum was measured at 400 MHz using tetramethyl silane in chloroform as reference (0 ppm).

^{13}C NMR (100 MHz) reactivity study in acetonitrile- d_3 (Figure S24):

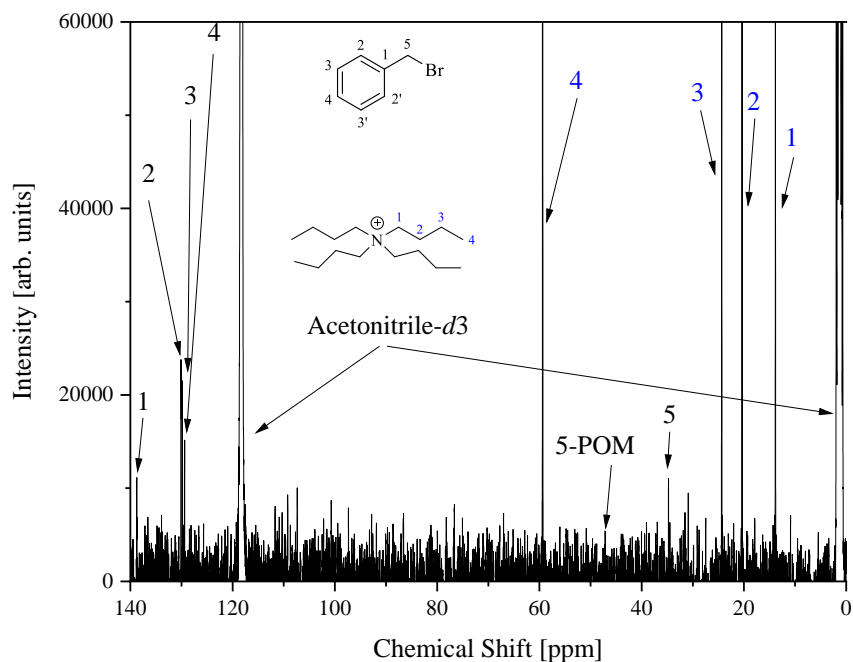


Figure S24: ^{13}C NMR of benzyl bromide and POM $n\text{Bu}_4\text{NPW}$ in acetonitrile- d_3 (reactivity study). The spectrum was measured at 100 MHz using tetramethyl silane in chloroform as reference (0 ppm).

^{31}P NMR (161.9 MHz) reactivity study in acetonitrile- d_3 (Figure S25):

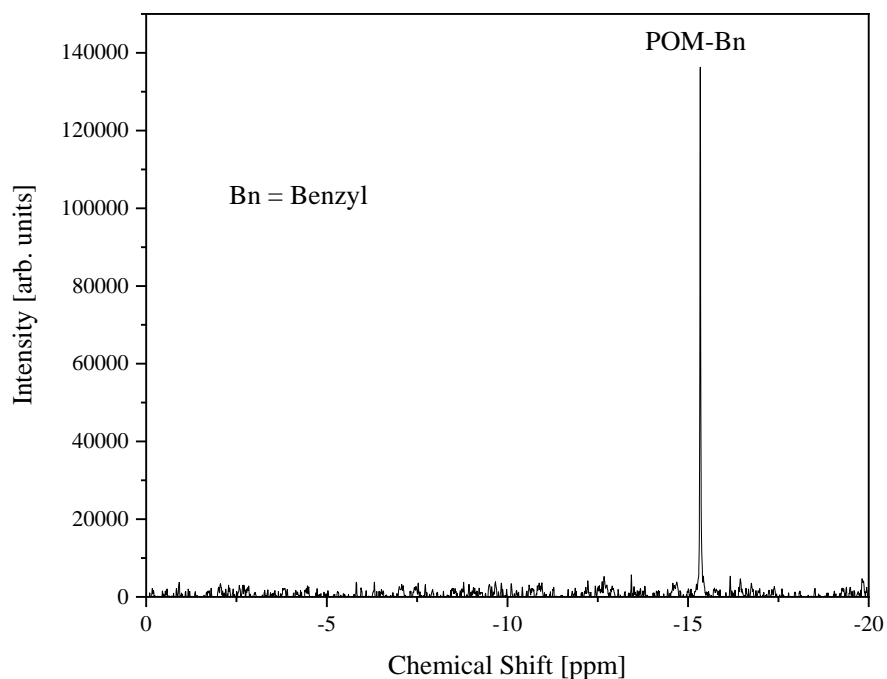


Figure S25: ^{31}P NMR of benzyl bromide and POM $n\text{Bu}_4\text{NPW}$ in acetonitrile- d_3 (reactivity study). The spectrum was measured at 161.9 MHz with aqueous H_3PO_4 solution as reference (0 ppm).

^1H NMR (400 MHz) reactivity study in acetonitrile- d_3 (Figure S26):

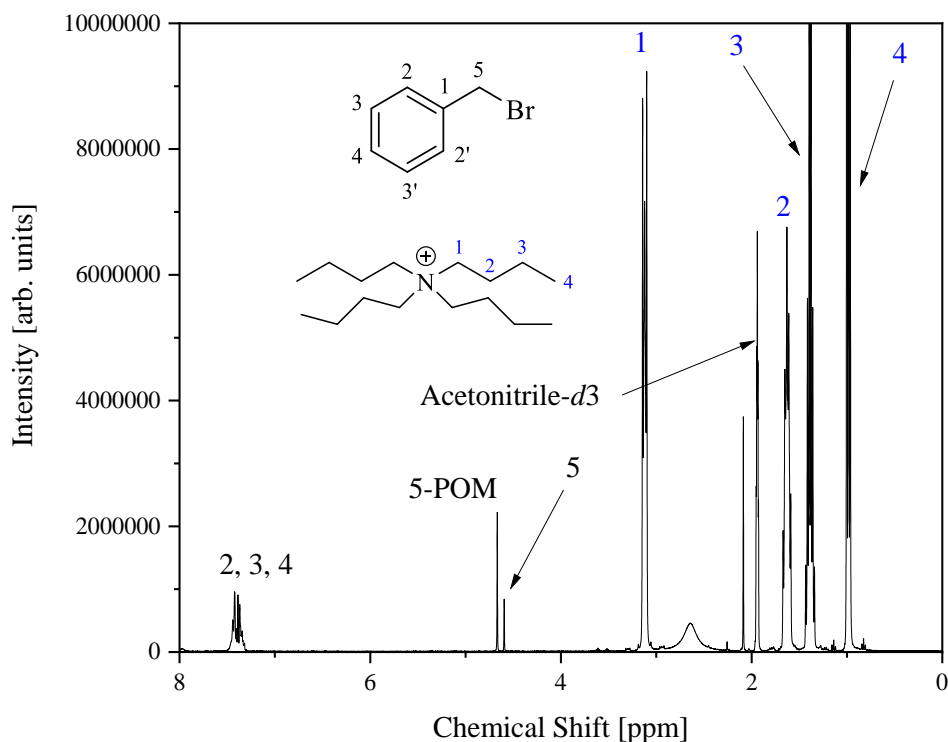


Figure S26: ^1H NMR of benzyl bromide and POM $n\text{Bu}_4\text{NPAIW}$ in acetonitrile- d_3 (reactivity study). The spectrum was measured at 400 MHz using tetramethyl silane in chloroform as reference (0 ppm).

^{13}C NMR (100 MHz) reactivity study in acetonitrile- d_3 (Figure S27):

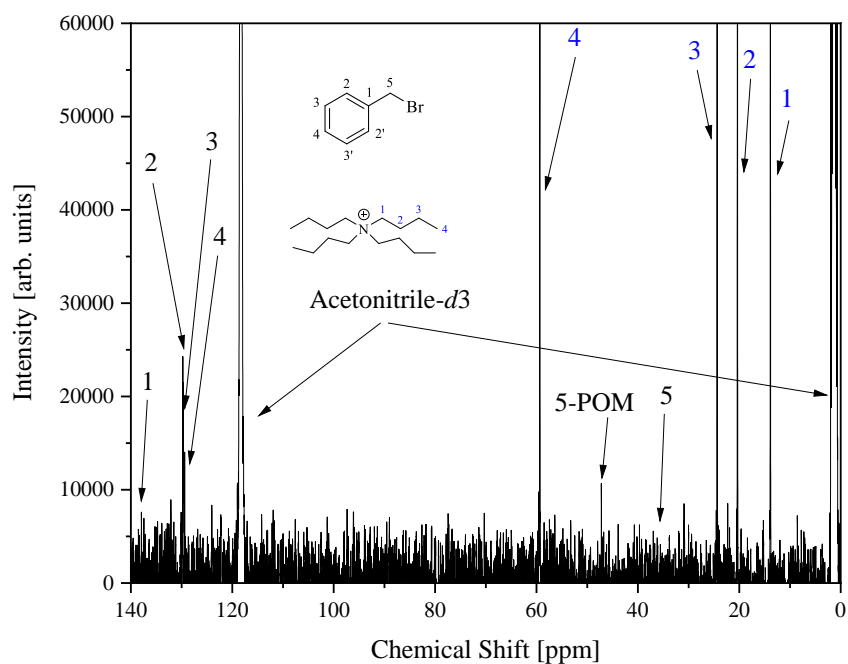


Figure S27: ^{13}C NMR of benzyl bromide and POM $n\text{Bu}_4\text{NPAIW}$ in acetonitrile- d_3 (reactivity study). The spectrum was measured at 100 MHz using tetramethyl silane in chloroform as reference (0 ppm).

^{31}P NMR (161.9 MHz) reactivity study in acetonitrile- d_3 (Figure S28):

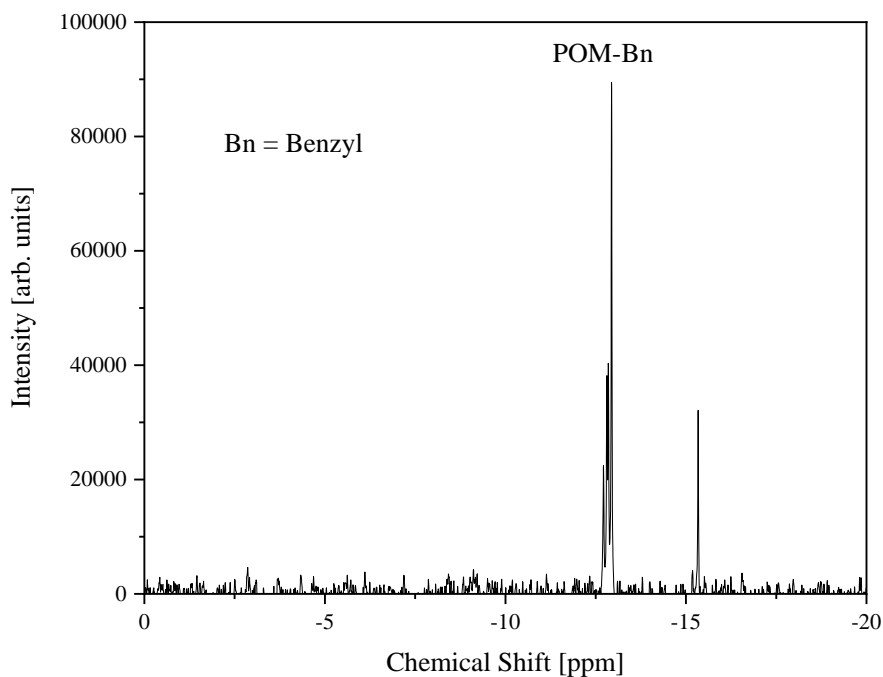


Figure S28: ^{31}P NMR of benzyl bromide and POM $n\text{Bu}_4\text{NPAIW}$ in acetonitrile- d_3 (reactivity study). The spectrum was measured at 161.9 MHz with aqueous H_3PO_4 solution as reference (0 ppm).

The ^{27}Al NMR data show that the Al species could be a tetrahedral coordinated AlO_4 species, indicating that the heteroelement was substituted with Al, see Figure S29.

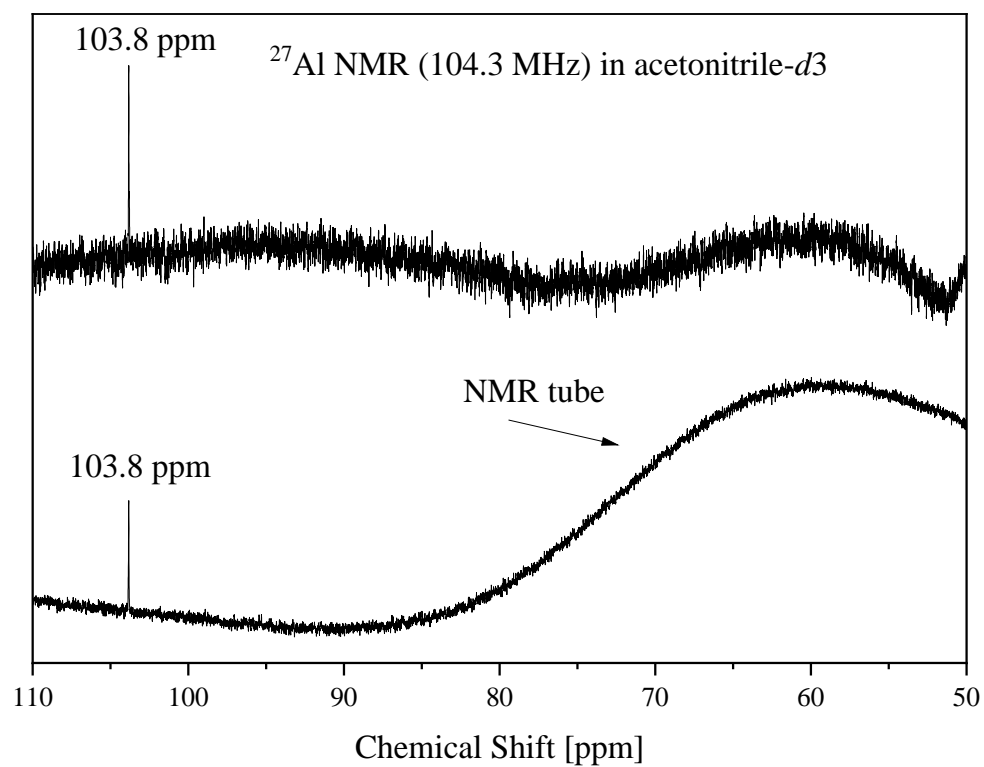


Figure S29: ^{27}Al NMR of compound **PAIW** in acetonitrile- d_3 , the sample was not entirely dissolved. The spectrum was measured at 104.3 MHz with aqueous $\text{Al}(\text{NO}_3)_3$ solution as reference (0 ppm).

2.3.5 Electrochemical Analysis

Cyclic voltammetry was conducted on a Pine Research WaveNow AFTP3 Potentiostat. For preparing the analyte solutions the following procedure was used: 10 mL of a 100 mmol/L solution of tetrabutylammonium hexafluorophosphate in acetonitrile was prepared and used for measuring the blank sample. The analyte was added, making sure that the analyte concentration is 1 mmol/L. A new measurement was done. In the last step ferrocene was added, making sure that the concentration is also 1 mmol/L. The measurement was repeated.

The following parameters were used in the software AfterMath 1.6.10515:

- Segments: 6
- Initial potential: 2 V
- Initial direction: falling
- Upper potential: 2 V
- Lower potential: -2 V
- Final potential: 2 V
- Sweep rate: 100 mV/s

The data were exported as .csv file and plotted in Origin 2019b.

The influence of element substitution on the electronic properties and the RedOx activity was analyzed by using electrochemical measurements, cyclic voltammetry (CV) and square-wave voltammetry (SWV). The data are illustrated in Figure S30. In a blank measurement an interference peak with unknown origin at -855.9 mV (SWV) was identified (in CV at -686.9 and -914.7 mV). Ferrocene was found at 514.7 mV (SWV) (in CV at 538.9 and 481.2 mV). Only in the SWV data a second peak for ferrocene was identified at -1696.6 mV. In general the RedOx activity of the POMs investigated in this work is less pronounced, which is in agreement with our results from our previous studies.^[13] For the POM anion **PW** a peak at -145.1 mV was found in the SWV data (in CV at -75.8 and -224 mV). This peak shifted to -224.8 mV (SWV) for POM **PAIW** and was found as a split band for **PSiW** at -260.1 and -169.8 mV (SWV). The discussed trend was only visible in the SWV data.

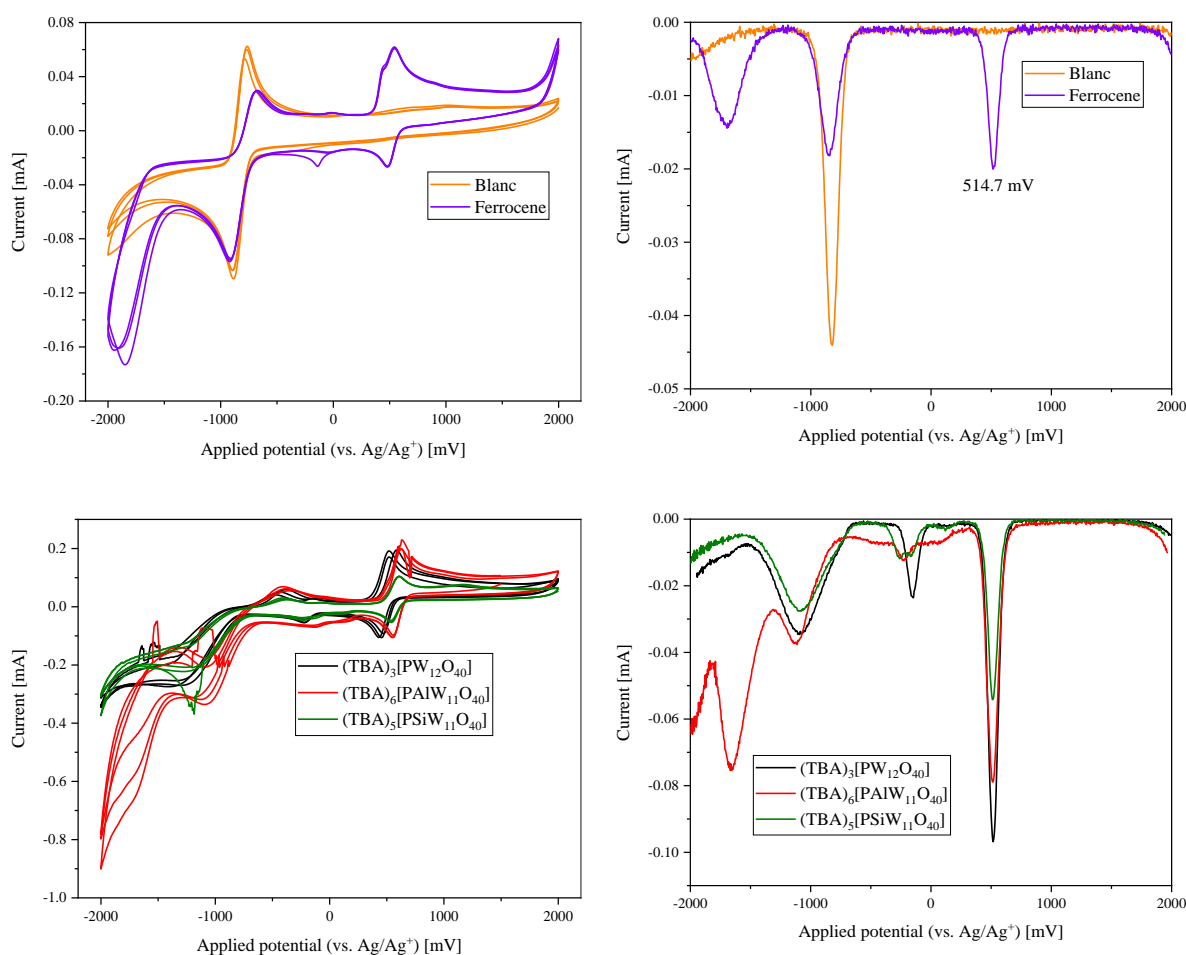


Figure S30: CV (left) and SWV measurements (right). Blanc measurements, containing pure solvent with supporting electrolyte and a ferrocene measurement (top) and measurements of the investigated POMs (bottom). All measurements were done in acetonitrile with tetrabutylammonium hexafluorophosphate as supporting electrolyte. Ferrocene was always used as reference.

From the electrochemical data it was shown that the RedOx properties are low pronounced and low influenced by foreign main-group element substitution. Therefore, these POMs are rather unsuitable for RedOx catalytic applications.

2.4 Computational chemistry

DFT calculations were conducted using Gaussian 16. The PBE1 functional and def2-svp basis set were used. All stationary points were confirmed as minima by vibrational analysis to confirm all modes were positive.

Figure S31 and S32 show the HOMO (left) and the HOMO-1 (right) molecular orbital of POM anion **PW** (Figure 31) and **AIW** (anion $[\text{AIW}_{12}\text{O}_{40}]^{5-}$) (Figure S32), that are delocalized over the entire cluster.

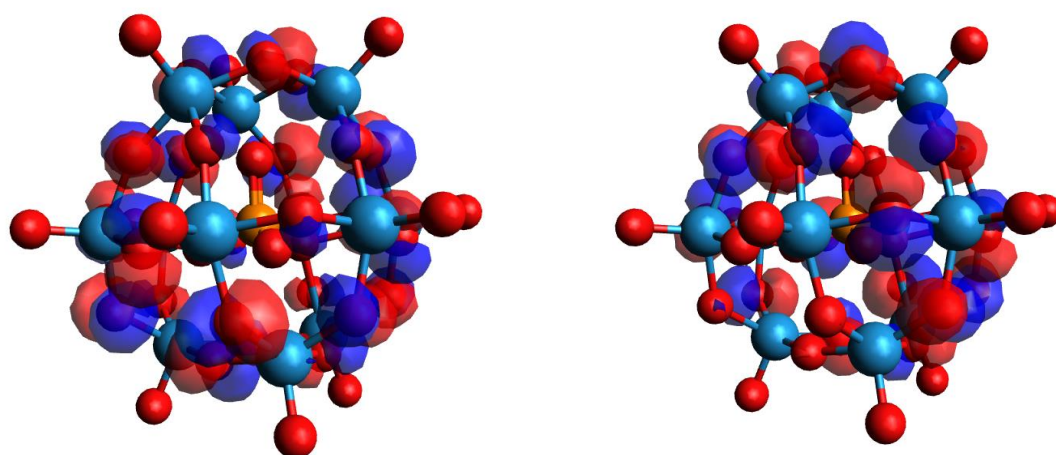


Figure S31: HOMO (left) and HOMO-1 (right) molecular orbital of POM anion **PW** with a delocalized molecular orbital over the cluster.

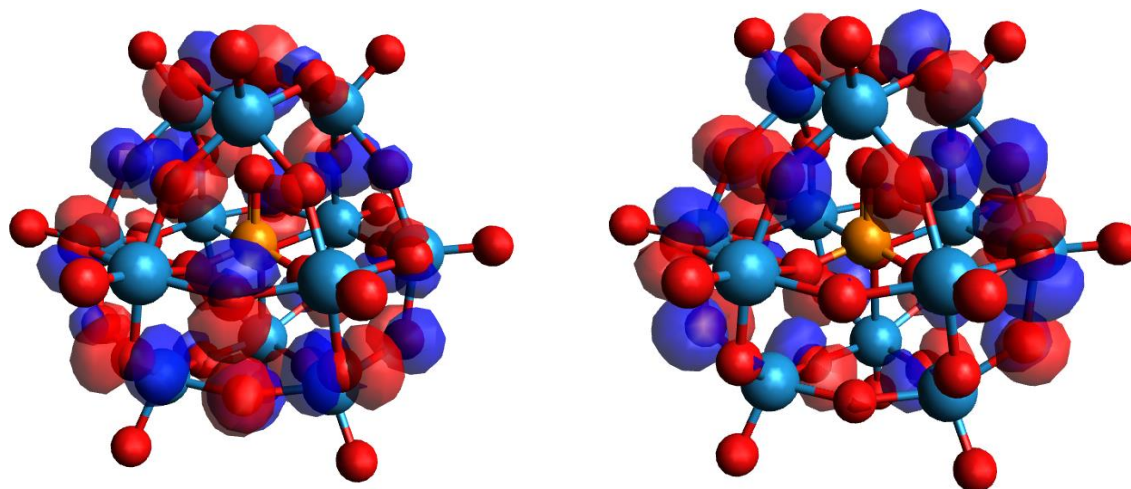


Figure S32: HOMO (left) and HOMO-1 (right) molecular orbital of POM anion **AIW** with a delocalized molecular orbital over the cluster.

Atomic coordinates:

POM anion [PW₁₂O₄₀]³⁻

W	8.29116	1.76109	3.10784
W	10.10067	3.55864	0.84064
W	11.44755	0.75113	4.64
W	10.78495	4.72989	7.78801
W	12.73293	6.67116	5.40867
W	7.91967	5.52644	6.16866
W	13.52633	3.10737	5.7962
W	8.78552	2.23573	6.6417
W	13.21273	2.65198	2.51354
W	7.61996	5.08108	2.52708
W	12.4885	6.16559	2.10303
W	9.9539	7.60915	3.77883
P	10.54971	4.17208	4.28519
O	9.54095	3.81511	3.17463
O	9.82442	4.17914	5.64587
O	11.14772	5.56675	4.00705
O	11.67292	3.12715	4.31409
O	7.01084	3.2815	2.72046
O	8.46776	4.75048	0.95931
O	8.90402	2.14679	1.2487
O	7.97802	2.08036	4.90079
O	7.38064	5.17419	4.52574
O	8.69696	6.61584	2.94397
O	11.03106	5.31734	1.06932
O	11.56677	2.76999	1.43174
O	9.87452	0.95799	3.46266
O	10.19253	1.29388	5.97011
O	7.52552	3.77732	6.87282
O	9.03735	7.00806	5.48246
O	11.17715	7.615	2.37188
O	13.2262	4.52766	2.26264
O	12.51872	0.94364	3.07695
O	12.87	1.27144	5.72362
O	9.80447	3.05195	8.02095
O	9.20714	5.66099	7.73491
O	11.43375	7.96353	5.0219
O	13.41142	6.85528	3.60187
O	14.2508	2.74638	4.01983
O	12.25821	3.47731	7.15171
O	11.75073	5.97179	6.8185
O	13.62379	4.93264	5.40776
O	7.25425	0.51816	2.74207
O	6.23701	5.81082	2.03989
O	10.17678	3.3918	-0.78251
O	7.94021	1.12212	7.50181
O	6.66885	6.35984	6.83448
O	9.38007	9.13541	3.68936

O	13.33519	6.86739	0.91367
O	14.28371	2.15022	1.40177
O	11.46781	-0.87865	4.81604
O	11.29961	4.97419	9.34923
O	13.8423	7.58925	6.14417
O	14.90742	2.89105	6.66255

POM anion [PAIW₁₁O₄₀]⁶⁻:

W	1.79645	2.51141	1.89558
W	1.84725	2.52352	-1.63907
W	-1.83208	2.48393	1.89831
W	-1.65842	-2.38431	2.22089
W	-1.71169	-2.63406	-1.58579
W	1.70209	-2.35704	2.21829
W	-3.59564	0.06284	0.12489
Al	0.00341	0.11399	4.11854
W	-1.89244	2.49198	-1.63682
W	3.59411	0.11987	0.11665
W	-0.00014	-0.22544	-3.41609
W	1.74941	-2.60788	-1.58862
P	0.00013	-0.03923	0.1409
O	1.26151	0.88105	0.11828
O	0.00885	-0.95313	1.37272
O	0.00652	-0.93681	-1.14221
O	-1.27653	0.85981	0.12044
O	3.41767	1.54308	1.37418
O	3.41255	1.45212	-1.26202
O	2.07161	3.331	0.00588
O	1.26599	1.28822	3.06518
O	2.95619	-1.0844	1.4281
O	2.96158	-1.17206	-1.15486
O	1.27446	1.06426	-2.80156
O	-0.02503	2.94877	-1.63718
O	-0.0229	3.06317	1.62883
O	-1.28247	1.26918	3.06795
O	1.3212	-1.32174	3.60998
O	1.66909	-2.93649	0.2186
O	1.3308	-1.5899	-3.22025
O	-1.29566	1.04368	-2.79906
O	-2.12416	3.29668	0.00847
O	-3.43972	1.48961	1.37965
O	-1.29255	-1.34267	3.61212
O	0.02891	-3.30596	2.33791
O	0.02565	-3.43143	-1.87041
O	-1.31015	-1.6103	-3.21766
O	-3.43894	1.39707	-1.25693
O	-2.93636	-1.13175	1.43314
O	-1.62033	-2.96331	0.22068
O	-2.94486	-1.21891	-1.14942

O	2.46589	3.78378	2.85108
O	5.29769	-0.14624	0.11784
O	2.4923	3.68392	-2.74168
O	0.00224	0.43298	5.74728
O	2.78368	-3.54145	2.86348
O	2.80703	-3.82745	-2.20062
O	-0.00372	0.01226	-5.1267
O	-2.55731	3.64203	-2.73849
O	-2.52025	3.74628	2.85386
O	-2.72045	-3.58545	2.86759
O	-2.75073	-3.87025	-2.19633
O	-5.29477	-0.23038	0.12925

POM anion $[\text{AlW}_{12}\text{O}_{40}]^{5-}$:

W	8.29116	1.76109	3.10784
W	10.10067	3.55864	0.84064
W	11.44755	0.75113	4.64
W	10.78495	4.72989	7.78801
W	12.73293	6.67116	5.40867
W	7.91967	5.52644	6.16866
W	13.52633	3.10737	5.7962
W	8.78552	2.23573	6.6417
W	13.21273	2.65198	2.51354
W	7.61996	5.08108	2.52708
W	12.4885	6.16559	2.10303
W	9.9539	7.60915	3.77883
Al	10.54971	4.17208	4.28519
O	9.54095	3.81511	3.17463
O	9.82442	4.17914	5.64587
O	11.14772	5.56675	4.00705
O	11.67292	3.12715	4.31409
O	7.01084	3.2815	2.72046
O	8.46776	4.75048	0.95931
O	8.90402	2.14679	1.2487
O	7.97802	2.08036	4.90079
O	7.38064	5.17419	4.52574
O	8.69696	6.61584	2.94397
O	11.03106	5.31734	1.06932
O	11.56677	2.76999	1.43174
O	9.87452	0.95799	3.46266
O	10.19253	1.29388	5.97011
O	7.52552	3.77732	6.87282
O	9.03735	7.00806	5.48246
O	11.17715	7.615	2.37188
O	13.2262	4.52766	2.26264
O	12.51872	0.94364	3.07695
O	12.87	1.27144	5.72362
O	9.80447	3.05195	8.02095
O	9.20714	5.66099	7.73491

O	11.43375	7.96353	5.0219
O	13.41142	6.85528	3.60187
O	14.2508	2.74638	4.01983
O	12.25821	3.47731	7.15171
O	11.75073	5.97179	6.8185
O	13.62379	4.93264	5.40776
O	7.25425	0.51816	2.74207
O	6.23701	5.81082	2.03989
O	10.17678	3.3918	-0.78251
O	7.94021	1.12212	7.50181
O	6.66885	6.35984	6.83448
O	9.38007	9.13541	3.68936
O	13.33519	6.86739	0.91367
O	14.28371	2.15022	1.40177
O	11.46781	-0.87865	4.81604
O	11.29961	4.97419	9.34923
O	13.8423	7.58925	6.14417
O	14.90742	2.89105	6.66255

POM anion [PSiW₁₁O₄₀]⁵⁻:

W	-1.81998	-2.49614	1.84249
W	-1.87739	-2.46942	-1.65361
W	1.80767	-2.50641	1.84076
W	1.68795	2.31203	2.22274
W	1.73683	2.63302	-1.54198
W	-1.66776	2.32404	2.22452
W	3.61347	-0.10528	0.11485
Si	0.00117	-0.1529	3.88599
W	1.85586	-2.48373	-1.65497
W	-3.61348	-0.08177	0.12262
W	-0.00054	0.27346	-3.39583
W	-1.72284	2.64285	-1.54018
P	0.00011	0.02233	0.11932
O	-1.27292	-0.87525	0.09221
O	0.004	0.92079	1.35879
O	0.0023	0.94462	-1.13847
O	1.26678	-0.8841	0.08965
O	-3.4319	-1.51162	1.37698
O	-3.4395	-1.40313	-1.2589
O	-2.1101	-3.29534	0.00489
O	-1.21413	-1.22659	2.98516
O	-2.94855	1.08508	1.46123
O	-2.95026	1.22356	-1.11288
O	-1.29103	-1.01234	-2.79822
O	-0.01102	-2.91629	-1.63865
O	-0.00864	-3.06293	1.59544
O	1.20834	-1.23098	2.98007
O	-1.22328	1.18961	3.5791
O	-1.63824	2.93637	0.30018

O	-1.31729	1.65893	-3.17504
O	1.28053	-1.02098	-2.80023
O	2.08931	-3.31006	0.00314
O	3.4239	-1.53273	1.37241
O	1.23644	1.18224	3.57852
O	0.01234	3.24032	2.39856
O	0.00936	3.45414	-1.77664
O	1.32421	1.65159	-3.17646
O	3.42745	-1.426	-1.26347
O	2.95685	1.06525	1.4564
O	1.65556	2.92467	0.29802
O	2.95804	1.20528	-1.11772
O	-2.47237	-3.7273	2.84413
O	-5.30499	0.20796	0.13339
O	-2.52378	-3.61522	-2.75651
O	0.00243	-0.53075	5.39831
O	-2.71819	3.46366	2.96637
O	-2.76129	3.8828	-2.11538
O	-0.00238	0.06393	-5.1011
O	2.49375	-3.6338	-2.7584
O	2.45246	-3.73993	2.84459
O	2.74653	3.4459	2.96203
O	2.78208	3.86706	-2.11765
O	5.30695	0.17279	0.124

3 Literature

- [1] R. G. Finke, M. W. Droege, P. J. Domaille, *Inorg. Chem.* **1987**, *26*, 3886–3896.
- [2] R. Calmanti, M. Selva, A. Perosa, *Mol. Catal.* **2020**, *486*, 110854.
- [3] H. G. O. Becker, W. Berger, G. Domschke, E. Fanghänel, J. Faust, M. Fischer, F. Gentz, K. Gewalt, R. Gluch, R. Mayer, K. Müller, D. Pavel, H. Schmidt, K. Schollberg, K. Schwetlick, E. Seiler, G. Zeppenfeld, R. Beckert, W. D. Habicher, P. Metz, *Organikum: Organisch-Chemisches Grundpraktikum*, Wiley-VCH Verlag, Weinheim, New York, Chichester, Brisbane, Singapore, Toronto, **2001**.
- [4] J. K. Lee, J. Melsheimer, S. Berndt, G. Mestl, R. Schlögl, K. Köhler, *Appl. Catal. A Gen.* **2001**, *214*, 125–148.
- [5] O. V. Dolomanov, L. J. Bourhis, R. J. Gildea, J. A. K. Howard, H. Puschmann, *J. Appl. Crystallogr.* **2009**, *42*, 339–341.
- [6] G. M. Sheldrick, *Acta Crystallogr. Sect. A Found. Crystallogr.* **2008**, *64*, 112–122.
- [7] C. B. Hübschle, G. M. Sheldrick, B. Dittrich, *J. Appl. Crystallogr.* **2011**, *44*, 1281–1284.
- [8] A. L. Spek, *Acta Crystallogr. Sect. D Biol. Crystallogr.* **2009**, *65*, 148–155.
- [9] A. L. Spek, *J. Appl. Crystallogr.* **2003**, *36*, 7–13.
- [10] A. L. Spek, *Acta Crystallogr. Sect. E Crystallogr. Commun.* **2020**, *76*, 1–11.
- [11] J. C. Raabe, J. Albert, M. J. Poller, *Chem. – A Eur. J.* **2022**, *28*, e202201084.
- [12] J.-C. Raabe, T. Esser, F. Jameel, M. Stein, J. Albert, M. J. Poller, *Inorg. Chem. Front.* **2023**, *10*, 4854–4868.
- [13] J.-C. Raabe, J. Aceituno Cruz, J. Albert, M. J. Poller, *Inorganics* **2023**, *11*, 138.
- [14] J.-C. Raabe, L. Hombach, M. J. Poller, A. Collauto, M. M. Roessler, A. Vorholt, A. K. Beine, J. Albert, *ChemCatChem* **2024**, *16*, DOI 10.1002/cctc.202400395.
- [15] P. Pyykkö, M. Atsumi, *Chem. - A Eur. J.* **2009**, *15*, 186–197.
- [16] Y. Jiang, S. Liu, S. Li, J. Miao, J. Zhang, L. Wu, *Chem. Commun.* **2011**, *47*, 10287.

[17] J.-C. Raabe, F. Jameel, M. Stein, J. Albert, M. J. Poller, *Dalt. Trans.* **2024**, 53, 454–466.

[18] I. V. Kozhevnikov, *Russ. Chem. Rev.* **1987**, 56, 811–825.